Spectral and Thermal Properties of Perchlorate Salts and Implications for Mars

Janice L. Bishop[1,2], Richard Quinn[1,2] and M. Darby Dyar[3]

[1]SETI Institute, Carl Sagan Center, Mountain View, CA, 94043

[2]NASA-Ames Research Center, Space Science and Astrobiology Division, Moffett Field, CA, 94035

[3]Mount Holyoke College, Department of Astronomy, South Hadley, MA, 01075

Keywords:

Perchlorate, Mars, reflectance spectroscopy, differential scanning calorimetry, hydrated salts

Revision 1

Revised and resubmitted to American Mineralogist February 28, 2014

Submitted to American Mineralogist August 9, 2013

Always consult and cite the final, published document. See http://www.minsocam.org or GeoscienceWorld

Abstract

K^+, Na^+, Ca^{2+}, Mg^{2+}, Fe^{2+}, Fe^{3+}, and Al^{3+} perchlorate salts were studied in order to provide spectral and thermal data for detecting and characterizing their possible presence on Mars. Spectral and thermal analyses are coordinated with structural analyses in order to understand how different cations and different hydration levels affect the mineral system. Near-infrared (NIR) spectral features for perchlorates are dominated by H_2O bands that occur at 0.978-1.01, 1.17-1.19, 1.42-1.48, 1.93-1.99, and 2.40-2.45 μm. Mid-IR spectral features are observed for vibrations of the tetrahedral ClO_4^- ion and occur as reflectance peaks at 1105-1130 cm^{-1} (~8.6-9 μm), 760-825 cm^{-1} (~12-13 μm), 630 cm^{-1} (~15.9 μm), 460-495 (~20-22 μm), and 130-215 (~50-75 μm). The spectral bands in both regions are sensitive to the type of cation present because the polarizing power is related to the band center for many of the spectral features. Band assignments were confirmed for many of the spectral features due to opposing trends in vibrational energies for the ClO_4^- and H_2O groups connected to different octahedral cations. Differential scanning calorimetry (DSC) data show variable patterns of water loss and thermal decomposition temperatures for perchlorates with different cations, consistent with changes in spectral features measured under varying hydration conditions. Results of the DSC analyses indicate that the bond energies of H_2O in perchlorates are different for each cation and hydration state. Structural parameters are available for Mg perchlorates (Robertson and Bish 2010) and the changes in structure due to hydration sate are consistent with DSC parameters and spectral features. Analyses of changes in the Mg perchlorate structures with H_2O content inform our understanding of the effects of hydration on other perchlorates, for which the specific structures are less well defined. Spectra of the hydrated Fe^{2+} and Fe^{3+} perchlorates changed

Always consult and cite the final, published document. See http://www.minsocam.org or GeoscienceWorld

significantly upon heating to 100 °C or measurement under low moisture conditions indicating that they are less stable than other perchlorates under dehydrated conditions. The perchlorate abundances observed by Phoenix and MSL are likely too low to be identified from orbit by CRISM, but may be sufficient to be identifiable by a VNIR imager on a future rover.

Introduction

Chlorine has long been known to be an important component of the Martian regolith, but the molecular form of this element was unknown (e.g., Clark et al. 1977; Clark et al. 2005). One of the achievements of the Phoenix mission was to identify perchlorate as the predominate form of soluble chorine in the regolith at the landing site (Hecht et al. 2009). Recent Phoenix Wet Chemistry Laboratory (WCL) measurements of soluble anions and cations indicate that the perchlorate anion is likely present at a level of 0.6 wt.% as a combination of $Ca(ClO_4)_2{\cdot}nH_2O$ and $Mg(ClO_4)_2{\cdot}nH_2O$ in the soil (Kounaves et al. 2014). Remote sensing analyses of soil features in 12 trenches observed with Phoenix's SSI Instrument found a band at 0.967 μm consistent with hydrated salts such as perchlorate (Cull et al. 2010b). Remote sensing studies by the Compact Reconnaissance Imaging Spectrometer for Mars (CRISM) of the Phoenix site with 18 m/pixel ground sampling show water ice (Cull et al. 2010a), but no evidence of perchlorate. Sample Analysis at Mars (SAM) results indicate the presence of Ca perchlorate at the Rocknest site in Gale Crater (Glavin et al. 2013; Leshin et al. 2013) and possibly Fe-perchlorates at the John Klein and Cumberland sites at Yellowknife Bay in Gale Crater (Ming et al. 2014).

At about the same time Phoenix identified perchlorates in the soil, orbital remote

Always consult and cite the final, published document. See http://www.minsocam.org or GeoscienceWorld

sensing analyses using thermal IR data led to the detection of a widespread region containing small chloride salt deposits with unusually high emissivity at shorter wavelengths in the southern highlands (Osterloo et al. 2008; Osterloo et al. 2010; Glotch et al. 2013). Most of these chloride-bearing outcrops occur in topographic lows and are attributed to brines formed in evaporitic environments. Anhydrous chloride salts are difficult to confirm on Mars using CRISM (Compact Reconnaissance Imaging Spectrometer for Mars), but have been identified at sites such as Terra Sirenum by a weaker 3 μm band and an increasing slope from 1 to 2.6 μm (Murchie et al. 2009; Wray et al. 2009). Analysis of the stratigraphy at these sites indicates that chloride deposits overlay ancient phyllosilicate outcrops (Murchie et al. 2009; Wray et al. 2009; Glotch et al. 2010); in some cases there is evidence that the salt deposits were mobilized by aqueous processes (Glotch et al. 2010). Mixtures of halite (NaCl) and basalt minerals match the observed spectral slope characteristic of these chloride deposits, with the most favorable results for halite grains in the 63-180 μm range (Jensen and Glotch 2011). The relationship of chlorides, perchlorates and other Cl compounds on Mars is unknown, however, they are observed together in cold desert sediments in the Antarctic Dry Valleys (Kounaves et al. 2010a) and thus could be related on Mars as well.

On Earth, perchlorate salts have been detected in the waters of ice-covered lakes of the Antarctic Dry Valleys, where they have been found to occur at 0.1-0.2 μg/L in many lakes but as high as 8 μg/L in one part of Lake Bonney (Jackson et al. 2012). Analyses of Atacama Desert samples revealed perchlorate in some regions up to levels as high as 42 μg/g (Parro et al. 2011). In rare cases that are limited to some Atacama nitrate deposits (Ericksen 1983), levels of naturally occurring perchlorate on Earth approach those found on Mars.

Always consult and cite the final, published document. See http://www.minsocam.org or GeoscienceWorld

Studies have shown that perchlorates on Earth are generally derived from reaction of atmospheric oxidants and Cl (Bao and Gu 2004; Michalski et al. 2004; Parker 2009; Kounaves et al. 2010b) and a similar process is thought to have occurred on Mars (Catling et al. 2010). However, photooxidation of Cl by oxide minerals in aqueous environments is another possible formation mechanism for perchlorate on early Mars (Schuttlefield et al. 2011).

Perchlorates have been identified on Mars by the WCL on Phoenix (Hecht et al. 2009; Kounaves et al. 2014) and SAM on MSL (Archer et al. 2013; Glavin et al. 2013; Leshin et al. 2013; Ming et al. 2014) and modeling of Viking, Thermal and Evolved Gas Analyzer (TEGA), and SAM results is consistent with perchlorate reacting with organics during thermal analysis (Navarro-Gonzalez et al. 2010; Glavin et al. 2013). However, the possibility of perchlorate induced combustion of soil organics combined with the presence of terrestrial organic contamination in the Viking GCMS and MSL SAM instruments has so far thwarted definitive identification of soil organics on Mars (e.g., Biemann and Bada 2011; Ming et al. 2014). Additionally, lower oxidation state oxychlorine compounds related to perchlorate may directly react with organics presence on the surface of Mars (Quinn et al. 2013).

Perchlorates and other chloride salts are highly deliquescent. The deliquescence of hygroscopic minerals such as chloride salts could allow for the occurrence of transient liquid water on Mars, even under the current arid climate (Renno et al. 2009; Davila et al. 2010; Gough et al. 2011) and perchlorates could represent a potential near-surface H_2O reservoir on Mars (Robertson and Bish, 2011). The visible/near-infrared (VNIR) spectral properties of perchlorates are dominated by features due to H_2O and differential scanning calorimetry (DSC) measures dehydration as well as phase changes. Because the number of

Always consult and cite the final, published document. See http://www.minsocam.org or GeoscienceWorld

H_2O molecules present in the unit formula for perchlorates determines the structure (Robertson and Bish 2010), the H_2O bond energies change as well as the spectral features and temperatures of dehydration. VNIR spectra are currently measured by CRISM in orbit around Mars and thermal properties were measured by TEGA on Phoenix. The purpose of this study is to present the spectral and thermal properties of several perchlorate salts in order to facilitate their detection on Mars.

Background

Structure and Bonding of Perchlorates

The perchlorate ion (ClO_4^-) forms stable complexes with a number of metals, especially in the absence of Cl^- or other halides; however, most are readily soluble in water (Michalski et al. 2013; Sowe et al. 2013). The metal perchlorate bond is largely covalent and usually weak (Michalski et al. 2013). Perchlorate ions can form structures with monodentate, bridging bidentate or chelating bidentate configurations (Olmstead et al. 1982; Horgan et al. 2013). The perchlorate ion is considered to be a strong oxidant; however it is thermally stable at Mars temperatures. Although it is difficult to chemically reduce perchlorate in aqueous solution, it can be reduced under some conditions by Ru^{2+} to the chlorate ion (ClO_3^-) and by Ti^{3+} and a few other rare metals to Cl^- (Michalski et al. 2013; Sowe et al. 2013). Perchlorate is not readily formed from chlorate in solution because the thermodynamically-favored disproportionation reaction of $4\ ClO_3^- = Cl^- + 3\ ClO_4^-$ proceeds very slowly, even at 100 °C (Sowe et al. 2013). Typically, perchlorates are synthesized by electrolytic oxidation of chlorates. Perchlorate anions have tetrahedral coordination polyhedra and solid perchlorates are generally isomorphous with salts of sulfates and

Always consult and cite the final, published document. See http://www.minsocam.org or GeoscienceWorld

other tetrahedrally coordinated anions (Sowe et al. 2013).

Crystal structures of perchlorates vary depending on the number of H_2O molecules per unit cell (e.g., Robertson and Bish 2010; Robertson and Bish 2011). Each Mg^{2+} cation is octahedrally-coordinated by some combination of bridging O^{2-} anions and H_2O. Through spectral analyses and symmetry considerations Ross (1962) determined that the ClO_4^- ions are connected to the metal cation via two O^{2-} anions. In the $Mg(ClO_4)_2{\cdot}6H_2O$ structure described by West (1935) every Mg^{2+} is bonded to six H_2O molecules. Robertson and Bish (2010) described the structures of multiple hydrated Mg perchlorates using a combination of an *ab initio* charge-flipping model based on x-ray powder diffraction data and subsequent fundamental-parameters Rietveld refinement. Analyses of Mg perchlorate at multiple hydration levels showed Mg^{2+} in octahedral coordination with H_2O molecules and ClO_4^- ions in different forms (Robertson and Bish 2010; Robertson and Bish 2011; Solovyov 2012).

i) For the hexahydrate state: six H_2O molecules are connected to Mg^{2+} and the ClO_4^- ions are H-bonded to the H_2O molecules.

ii) For the tetrahydrate state: four H_2O molecules and two ClO_4^- ions are connected to the Mg cation with the large tetrahedrally-coordinated perchloride ions positioned in a *trans* arrangement at opposite ends of the octahedron with space group *C2*.

iii) For the dihydrate state: two H_2O molecules and 4 ClO_4^- ions are connected to the Mg cation giving space group *C2/m*.

Models of the $Mg(ClO_4)_2{\cdot}4H_2O$ and $Mg(ClO_4)_2{\cdot}2H_2O$ structures from Robertson and Bish (2010) are shown in Figures 1 and 2. Skogareva et al. (2012) also published the crystal

Always consult and cite the final, published document. See http://www.minsocam.org or GeoscienceWorld

structure of the trivalent iron perchlorate, $(Fe(H_2O)_6)^{3+}(ClO_4)_3 \cdot 3H_2O$. That structure contains two Fe cation sites, both of which are bonded to six H_2O molecules each.

Low temperature studies of $Mg(ClO_4)_2 \cdot 6H_2O$ found at least eight distinct types of H_2O and multiple types of H cations with variable charge densities below 108 K, where a phase transition occurs (White and Falk 1986). This indicates a complex low-temperature structure. Above this transition there are only two types of H cations that were assigned to inequivalent sites in the H_2O molecules (White and Falk 1986). All H cations became equivalent after a phase change at 273 K and then the perchlorate ions became increasingly disordered following another phase change at 325 K (White and Falk 1986). Experiments under low P_{H2O} showed that $Mg(ClO_4)_2 \cdot 6H_2O$ is the stable phase at 273 K and that it resisted dehydration at low temperatures and didn't dehydrate until 323 K (Robertson and Bish 2010), consistent with the phase change observed at 325 K by White and Falk (1986). Robertson and Bish (2010) suggest that transitions occur with thermal decomposition in the Mg perchlorate hydrate system from a structure involving isolated polyhedra for $Mg(ClO_4)_2 \cdot 6H_2O$, to isolated clusters for $Mg(ClO_4)_2 \cdot 4H_2O$, to chains for $Mg(ClO_4)_2 \cdot 2H_2O$, and an infinite framework for anhydrous $Mg(ClO_4)_2$.

Deliquescence and Efflorescence of Perchlorates

Perchlorates are highly hygroscopic and readily transform from a crystalline solid to aqueous state (deliquescence) under humid conditions. Recent experiments and modeling work provide constraints on the geochemical conditions governing deliquescence and efflorescence (transformation from a liquid state to a crystalline solid) of perchlorates (Chevrier et al. 2009; Davila et al. 2010; Marion et al. 2010; Gough et al. 2011). Modeling by

Always consult and cite the final, published document. See http://www.minsocam.org or GeoscienceWorld

Marion et al. (2010) indicates that Na and Mg perchlorate were more likely to have precipitated at the Phoenix landing site than Ca perchlorate because Ca would have preferentially formed calcite and gypsum. The eutectic points were modeled at ~239 K for $NaClO_4 \cdot 2H_2O$, ~205 K for $Mg(ClO_4)_2 \cdot 6H_2O$, and ~199 K for $Ca(ClO_4)_2 \cdot 8H_2O$ (Marion et al. 2010) using data from Pestova et al. (2005). However, re-analysis of the Wet Chemistry Lab data on Phoenix support Ca perchlorate as the dominant salt in the soil (Kounaves et al. 2012; Kounaves et al. 2014). Davila et al. (2010) modeled the temperatures and relative humidity (RH) on Mars and determined that many Cl salts would deliquesce on Mars, resulting in transient Cl brine solutions on Mars today.

Gough et al. (2011) studied the stability of $Mg(ClO_4)_2 \cdot 6H_2O$, $NaClO_4$ and $NaClO_4 \cdot H_2O$ over the range 223-273 K and variable RH conditions and found that their data were consistent with the modeling results of Chevrier et al. (2009). $Mg(ClO_4)_2 \cdot 6H_2O$ deliquesces at 55 %RH at 223 K and at 42 %RH at 273 K, while $NaClO_4 \cdot H_2O$ deliquesces at 64 %RH at 228 K and at 51 %RH at 273 K. Similarly, Nuding et al. (2013) studied $Ca(ClO_4)_2$ and found that deliquescence occurred at 55 %RH at 223 K and at 23 %RH at 263 K. They also observed that higher hydration states of Ca perchlorates are less deliquescent. Efflorescence occurred at much lower RH levels for perchlorates and was largely independent of temperature: ~19 %RH for $Mg(ClO_4)_2 \cdot 6H_2O$ (Gough et al. 2011), ~13 %RH for $NaClO_4$ (Gough et al. 2011), and ~16 %RH for $Ca(ClO_4)_2$ (Nuding et al. 2013). This hysteresis effect could result in metastable, supersaturated perchlorate salt solutions on Mars today (Gough et al. 2011). The Na perchlorate solution only formed anhydrous $NaClO_4$ from solution and hydration of $NaClO_4$ is very slow. Thus, on Mars either anhydrous $NaClO_4$ salt or $NaClO_4$ solution is more likely to be present than a hydrated form of Na

Always consult and cite the final, published document. See http://www.minsocam.org or GeoscienceWorld

perchlorate (Gough et al. 2011). At ~250 K water activity levels increase for the Ca perchlorate system from 0 for the anhydrous form to ~0.25 for $Ca(ClO_4)_2 \cdot 4H_2O$ and to ~0.4 for $Ca(ClO_4)_2 \cdot 8H_2O$ (Nuding et al. 2013).

Spectral Properties of Perchlorates

Perchlorate salts have been the focus of several transmittance IR studies (Miller and Wilkins 1952; Miller et al. 1960; Ross 1962; Nebgen et al. 1966; Gadsden 1975; Lewis et al. 1975; White and Falk 1986; 2002; Chen et al. 2004; Weitz et al. 2013). Hathaway and Underhill (1961) found that isolated ClO_4^- ions have *Td* symmetry (*T*2 modes are active), unidentate ClO_4 coordination has *C3v* symmetry (*A*1, *E* and *A*1+*E* modes active), and bidentate ClO_4 coordination has *C2v* symmetry (*A*1, and *A*1+*B*1+*B*2 modes active). The perchlorate ion has bands near 1100 and 620 cm^{-1} due to the *T*2, *A*1+*E*, and *A*1+*B*1+*B*2 modes (Ross 1962; Lewis et al. 1975; Weitz et al. 2013). Additional bands are observed near 930 cm^{-1} for the *A*1 mode and near 500 cm^{-1} for the *E* mode. Further, the *A*1+*E* modes in unidentate perchlorates with *C3v* symmetry show variation in the position of the 600-650 cm^{-1} band depending on the type of cation (Lewis et al. 1975).

Mid-IR transmission spectra of ClO_4^- ions exhibit vibrational bands near 620 and 1100 cm^{-1}, while the chlorate ClO_3^- ions have bands at 1000-1100, 620, and 450-500 cm^{-1} (Gadsden 1975). A nitronium perchlorate IR and Raman study assigned an asymmetric stretch for the ClO_4^- ion at 1082-1143 cm^{-1}, a symmetric stretch at 936 cm^{-1}, an asymmetric bend at 625 cm^{-1}, and a symmetric bend (Raman only) at 461 cm^{-1} (Nebgen et al. 1966). The asymmetric stretching band shifts with cation type and was observed near 1100 cm^{-1} for Na perchlorate, as a doublet at 1075 and 1140 cm^{-1} for K perchlorate and as a doublet at

Always consult and cite the final, published document. See http://www.minsocam.org or GeoscienceWorld

1060 and 1130 cm^{-1} for Mg perchlorate (Miller and Wilkins 1952). The symmetric stretch has been observed at 940 cm^{-1} for K perchlorate and as a doublet at 945 and 962 cm^{-1} for Mg perchlorate (Miller and Wilkins 1952). The asymmetric bend was observed at 624 cm^{-1} for Na perchlorate, 625 cm^{-1} for K perchlorate and at 622 cm^{-1} for Mg perchlorate (Miller et al. 1960). Weak bands were also observed near 480-495 cm^{-1} for a few perchlorates, which is consistent with some chlorate being present in the samples (Miller et al. 1960). Presumably, the symmetry change from ClO_4^- to ClO_3^- allows the symmetric bending vibration to become IR active. Chlorates have *C3v* symmetry and exhibit bending vibrations at 480-510 cm^{-1} and 615-630 cm^{-1} (Miller et al. 1960), and stretching vibrations at 913-990 cm^{-1} (Miller and Wilkins 1952). The vibrational bands measured in transmittance spectra of perchlorates and chlorates are summarized in Table 1. ATR studies of perchlorate solutions found that the asymmetric stretching band (ν_3) shifted towards lower frequencies (longer wavelengths) with increasing perchlorate concentration, while the position of the symmetric stretching band (ν_1) did not shift with perchlorate concentration (Chen et al. 2004). Kloprogge et al. (2002) noted similarities in the IR and Raman vibrations of SO_4^{2-} and ClO_4^- molecules present in the interlayer region of hydrotalcite due to similarities in the tetrahedral bonding of these molecules. These interlayer ClO_4^- molecules exhibited transmission IR absorptions at 626-635 cm^{-1} for ν_4, 935 cm^{-1} for ν_1 and 1096-1145 cm^{-1} for ν_3 (Kloprogge et al. 2002). Free ClO_4^- molecules with *T*d symmetry only have spectral absorptions for the ν_4 and ν_3 vibrations at 645 and 1128 cm^{-1} (Ross 1962; Ross 1972). Peak positions in transmittance spectra of minerals differ from those observed in reflectance and emissivity spectra because transmittance spectra are a

Always consult and cite the final, published document. See http://www.minsocam.org or GeoscienceWorld

function of absorbance only, while reflectance and emissivity spectra depend on both absorbance and scattering properties (e.g., Mcmillan and Hofmeister 1988).

Additional IR bands are observed for perchlorate salts due to H_2O molecules. A band at 3580 cm^{-1} (~2.79 μm) is assigned to H_2O H-bonded to ClO_4^- in an ATR study and does not vary with cation (Chen et al. 2004). Another band is observed at 3196 cm^{-1} (~3.13 μm) for Na perchlorate and 3254 cm^{-1} (~3.07 μm) for Mg perchlorate that varies with differences in polarization of the cation (Chen et al. 2004). Near-IR reflectance spectra of Mg perchlorates and other Cl salts show differences in the H_2O bands as a function of the hydration level of the salt (Hanley et al. 2010; Hanley et al. 2011), which are likely due to structural changes as shown in Figures 1-2 and by Robertson and Bish (2010).

Low temperature experiments were performed with Ca perchlorate solutions in order to study spectral changes as the liquid changed to a glassy state (Kanno and Hiraishi 1981). These studies of H-bonding in Ca perchlorates at 77 K show that additional H_2O stretching bands are present near 3545 cm^{-1} (~2.82 μm) in Raman spectra of a hydrated glassy low temperature perchlorate system in addition to the H_2O stretching band observed near 3585 cm^{-1} (~2.79 μm) for hydrated perchlorate solution (Kanno and Hiraishi 1981). These were assigned to OH/H_2O groups weakly H-bonded to perchlorate ions (e.g., Adams et al. 1971).

Methods

Perchlorate samples in this study were obtained from Sigma Aldrich and were reported to be 98-99% pure. The Na and K perchlorates were anhydrous. The Mg perchlorate is not described as having any water, but H_2O is clearly present in the data and the sample must

Always consult and cite the final, published document. See http://www.minsocam.org or GeoscienceWorld

be hydrated. The Fe^{2+} and Fe^{3+} perchlorates are described as hydrated without providing information on how many waters are expected per formula unit. The Ca perchlorate is described as $Ca(ClO_4)_2{\cdot}4H_2O$ and the Al perchlorate is described as $Al(ClO_4)_3{\cdot}9H_2O$. The Na, K, Ca, Mg and Al perchlorates are all white, the Fe^{2+} perchlorate is pale green, and the Fe^{3+} perchlorate is pale orange to yellow.

Measurement of reflectance spectra

Reflectance spectra were measured in a horizontal sample dish using an ASD spectrometer under ambient conditions at the SETI Institute, using a bidirectional VNIR spectrometer under ambient conditions at Brown University's RELAB (Pieters 1983), and using a biconical Nicolet FTIR spectrometer in a controlled, dry environment at RELAB (e.g., Bishop et al. 1995). The SETI Institute measurements included acquiring spectra of the perchlorates as received and then again following short-term heat treatments at 100 °C. The samples in these experiments were heated in an oven in room air for 10-20 minute intervals, removed from the oven for a few minutes for spectral measurements and then in some cases returned to the oven for continued heating at 100 °C.

Ambient spectra in both labs were measured relative to Halon from 0.3 to 2.5 μm. Infrared reflectance spectra were measured relative to a rough gold surface with 2 cm^{-1} spectral sampling from 1-50 μm in an environment purged of H_2O- and CO_2- for 10-12 hours as in past studies (e.g. Bishop et al. 1995). Composite, absolute reflectance spectra were prepared by scaling the FTIR data to the bidirectional data near 1.2 μm. Additional FTIR spectra were collected following measurement of the IR spectra in three spectral regions (including some heating of the sample during measurement) and extended

Always consult and cite the final, published document. See http://www.minsocam.org or GeoscienceWorld

exposure to the dehydrated environment of the sample chamber. For some samples heating by the FTIR beam and/or longer exposure to the dehydrated conditions in the H_2O-purged environment resulted in changes to the spectral features.

Measurement of DSC data

Differential scanning calorimetry (DSC) scans were obtained using a Perkin-Elmer Pyris calorimeter. Perchlorate samples weighing from 5 to 10 mg were crimp sealed in standard 40 µl Perkin-Elmer aluminum pans with covers. Samples were analyzed over a temperature range of 20 °C up to a maximum of 600 °C at a scan rate of 20 °C/min. A nitrogen purge gas (99.999% purity) at 1 bar with a flow rate of 20 cc/min was used.

Results and Discussion

VNIR Reflectance Spectra

Visible/near-infrared (VNIR) spectra of perchlorates are dominated by combinations and overtones of the H_2O vibrations near 1.42-1.48, 1.93-1.98, and 2.7-2.78 µm (Figure 3, Table 2). Spectra of the K and Na perchlorates in our study do not exhibit these bands, confirming their anhydrous form. Iron perchlorates have additional absorptions due to electronic excitations (e.g., Burns 1993). These bands are broader than the vibrational features and occur near 0.767 µm for Fe^{3+} perchlorate and near 0.95-1.1 µm for Fe^{2+} perchlorate. Overtones and combinations of the ClO_4^- vibrations are observed near 3.2-4 µm and are most prominent in the spectra of the K and Na perchlorate (Figure 3).

The band centers near 1.4, 1.9 and 2.7 µm all shift in similar ways (Figure 4) with the

Always consult and cite the final, published document. See http://www.minsocam.org or GeoscienceWorld

octahedral cation such that the vibrational energy depends on the polarizing power of the cation and structure of the solid. Polarizing power is the charge divided by the effective ionic radius and is also termed charge density or ionic potential (e.g., Huheey et al. 1993). Polarizing power was determined for the cations in the perchlorates of our study and follows the trends: Al>Fe^{3+}>Mg>Fe^{2+}>Ca>Na>K (Table 2). These values were compared with the putative water vibrations to confirm their assignment (Figure 5).

For the polyhydrated perchlorate structure the H_2O stretching vibration changed from 3610 cm^{-1} for Mg, to 3615 cm^{-1} for Fe^{2+}, to 3530 cm^{-1} for Fe^{3+}, to 3540 cm^{-1} for Al (Table 2), which compares well with the polarizing power of these cations. Similar trends were observed for the H_2O stretching overtone near 1.43-1.48 μm (6775-6970 cm^{-1}) and the H_2O combination stretching plus bending band near 1.93-1.99 μm (5025-5180 cm^{-1}). The $Ca(ClO_4)_2{\cdot}4H_2O$ spectrum exhibits two H_2O stretching vibrations at 3655 and 3585 cm^{-1} due to different H_2O sites in the structure as shown for Mg perchlorate in Figure 1. The $Ca(ClO_4)_2{\cdot}4H_2O$ spectrum also includes a doublet at 1.75 and 1.80 μm that is not observed for the other perchlorates in our study. These are attributed to overtones and combinations of H_2O vibrations in a constrained structure such as the isolated polyhedral in tetrahydrated perchlorates. Related features near 1.75-1.76 and 1.79-1.82 μm were observed in spectra of $Mg(ClO_3)_2{\cdot}2H_2O$, $MgCl_2{\cdot}2H_2O$, and $CaCl_2{\cdot}2H_2O$ (Hanley et al. 2010; Hanley et al. 2011), supporting the assignment of these features to H_2O in a constrained environment.

VNIR Reflectance Spectra Under Changing Hydration Environments

In order to evaluate changes in the spectral properties with hydration level, reflectance

Always consult and cite the final, published document. See http://www.minsocam.org or GeoscienceWorld

spectra of the samples were measured under differing environmental conditions. The K, Na and Mg perchlorate samples each converted to a liquid after heating for 10 minutes in an oven with room air at 100 °C, so reflectance spectra were not measured after heating for these samples. Because 100 °C is below their melting points, these samples may have gained H_2O and deliquesced. In contrast, the K, Na and Mg perchlorate samples did not liquefy after 10+ hours of exposure to H_2O-purged conditions inside the Nicolet spectrometer. Reflectance spectra measured of these samples after purging out the H_2O for ~10 hours showed virtually no changes relative to spectra measured again following an additional few hours in the chamber and heating by the FTIR beam. In different experiments by Morris et al. (2009) spectra of $Mg(ClO_4)_2 \cdot 6H_2O$ exhibited small reductions in hydration bands after heating at 210 °C in dry N_2 and large reductions in hydration bands after heating to 330 °C (Morris et al. 2009).

The spectrum of Ca perchlorate exhibited almost no change after heating for 10 minutes in an oven with room air at 100 °C, but did show some decrease in intensity of the H_2O bands following dehydration and heating by the FTIR beam in the H_2O-purged environment of the Nicolet spectrometer. This suggests that either 10 minutes at 100 °C were insufficient to dehydrate the sample or it rehydrated within the few minutes required to run the spectra. The Fe^{2+}, Fe^{3+} and Al perchlorates did change upon dehydration and heating and spectra of these samples under different conditions are shown in Figure 6.

Spectra of $Fe^{3+}(ClO_4)_3 \cdot nH_2O$ shown in Figure 6a exhibit the strongest H_2O band for the spectra measured under ambient conditions. This sample was pale orange in color, but changed to bright orange after heating 10 minutes at 100 °C. The reflectance is 10-20% brighter, but the H_2O overtone and combination bands near 1.46 and 1.98 μm appear about

Always consult and cite the final, published document. See http://www.minsocam.org or GeoscienceWorld

the same intensity and the broad water saturation past 1.5 μm is unchanged. This suggests that the sample either did not dehydrate after heating 10 minutes or it rehydrated within the few minutes required to run the spectra. After removing the sample from the oven for ~10 minutes and heating the sample for an additional 20 minutes at 100 °C, the crystals partially melted and turned white, which could indicate a change to a different structure. The spectrum of this sample heated for 10 and then 20 minutes is about twice as bright as the original spectrum and the H_2O bands are sharper and shifted to 1.45 and 1.96 μm. A new weak feature appeared in the spectrum as well at 2.18 μm. This is consistent with a phase change. Spectra measured after dehydrating the samples 10+ hours in the spectrometer chamber (where H_2O is pumped out of the environment) resulted in bands near 1.46 and 1.98 μm, and some reduction in the broad water saturation past 1.5 μm. Subsequent measurements after heating the sample with the IR beam and continued exposure to the low humidity environment produced a spectrum with bands again at 1.46 and 1.98 μm and further reduction in the broad water saturation past 1.5 μm. Thus, it appears that reducing the humidity level in the FTIR spectrometer experiments decreased the adsorbed water in the system, but did not cause a phase change. In contrast, heating the sample for 10+20 minutes at 100 °C did cause a structural change that produced a different color and shift in the wavelength of the H_2O bands. Neither the Fe^{3+} electronic excitation absorption at 0.76 μm, nor the reflectance maximum near 0.62 μm changed, but the shoulder near 0.45-0.5 μm changed shape slightly as the color changed.

Spectra of $Fe^{2+}(ClO_4)_2 \cdot nH_2O$ in Figure 6b show strong H_2O overtone and combination bands that are similar to those observed for the Fe^{3+} perchlorate. The H_2O stretching overtone occurs at 1.44 μm in these spectra and the H_2O stretch + bend combination band

Always consult and cite the final, published document. See http://www.minsocam.org or GeoscienceWorld

occurs at 1.95 μm; neither appeared to change wavelength as the sample was heated. A weak band is observed at 2.16 μm in all the spectra and is more clearly present in spectra of the heated samples. Spectra of the heated and dehydrated samples are less saturated from 1.5-2.5 μm and all of the bands in this region are better resolved. The shape of the strong crystal field transition absorption near 0.97 μm appears to change on the long wavelength side of the band as the sample is dehydrated, but this may be due to variations in the intensities of the H_2O overtones near 1.0-1.17 μm, rather than changes in the Fe^{2+} electronic excitation. However, the reflectance minimum near 0.55 μm in the ambient spectrum shifted toward longer wavelengths with heating as the color changed from pale green to orange and then dark orange. The spectrum of the sample heated for 10 minutes at 100 °C (changed from pale green to partly orange) has a reflectance maximum at 0.62 μm as does the Fe^{3+} perchlorate spectrum, but there is no Fe^{3+} electronic excitation absorption at 0.76 μm as would be expected if the whole sample had been oxidized. The reflectance maximum occurred at 0.70 μm for the Fe^{2+} perchlorate sample heated for 10+20+30 minutes.

Spectra of $Al(ClO_4)_3{\cdot}9H_2O$ in Figure 6c show strong H_2O overtone and combination bands and the spectrum measured under ambient conditions is largely saturated past 1.5 μm, similar to what was observed for Fe^{3+} perchlorate. The reflectance was brighter for the sample heated at 100 °C for 10 minutes and the saturation decreased slightly. Upon dehydration in the FTIR spectrometer, the saturation decreased further and the H_2O bands near 1.48 and 1.97 μm are readily observable.

Differential Scanning Calorimetry Data

Always consult and cite the final, published document. See http://www.minsocam.org or GeoscienceWorld

DSC data are shown for the K^+, Na^+, Mg^{2+}, Fe^{2+} and Fe^{3+} perchlorates in Figure 7. The scan of the anhydrous $KClO_4$ (Figure 7a) shows an endothermic peak with an onset of ~300 °C due to the transition from rhombic to cubic structure. This transition is followed by an endothermic peak due to the fusion of the salt (onset 585 °C) that occurs just prior to the onset of the exothermic decomposition at ~600 °C. Similar to $KClO_4$, the $NaClO_4$ DSC scan (Figure 7b) shows an endothermic peak with an onset at 307 °C due to a solid-phase transition (orthorhombic to cubic), an endothermic salt fusion peak (melting) with an onset at 467 °C followed by a broad exothermic decomposition peak. Very small endotherms observed at 41 °C and 88 °C may indicate trace amounts of water in the $KClO_4$ sample. $NaClO_4$ monohydrate has been reported to dehydrate in two stages with the release of $0.2H_2O$ and $0.8H_2O$ (per mole) at 60°C and 150°C respectively (Devlin and Herley 1987). These water endotherms are not observed in our $NaClO_4$ DSC scans.

The $Mg(ClO_4)_2{\cdot}6H_2O$ scan (Figure 7c) shows three broad dehydration steps each corresponding to the loss of two H_2O (Delvin and Herley 1986). The onsets for the first two dehydration endotherms occur at ~135 °C and ~240 °C, followed by a complex final dehydration endotherm that is completed by ~370 °C. Dehydration is followed by the stepwise decomposition of $Mg(ClO_4)_2{\cdot}2H_2O$. $Ca(ClO_4)_2{\cdot}4H_2O$ shows an endothermic loss of water over a broad temperature range with dehydration ending at ~320 °C. Dehydration of this sample is followed by a sharp exothermic peak at 348 °C, likely due to a phase transition. The onset of decomposition is seen at ~460 °C (Figure 7d).

In comparison to K^+, Na^+, Ca^{2+}, and Mg^{2+} perchlorates, the decomposition of Fe^{2+} and Fe^{3+} occurs at a low temperature (~125-150 °C) and is followed by a complex endotherm that is likely due to sample dehydration.

Always consult and cite the final, published document. See http://www.minsocam.org or GeoscienceWorld

Mid-IR Reflectance Spectra

The mid-IR reflectance spectral properties of perchlorates in our study are related to the bands observed for transmittance IR spectra of perchlorates in past studies (Table 1), and to reflectance (Bishop and Murad 1996; Bishop and Murad 2005) and emittance (Lane 2007) spectra of sulfates. The reflectance peaks described here would occur as emissivity minima. The ν_3 asymmetric stretch near 1100-1200 cm^{-1} (8-9 μm) and ν_4 asymmetric bend near 630 cm^{-1} (~16 μm) are observed for all our perchlorate spectra (Figures 8-9, Table 2). The ν_1 and ν_2 vibrations were also observed for the anhydrous perchlorates, suggesting that their structures are disrupted enough to enable these modes to become IR active. The ν_4 band was observed at 630 cm^{-1} for all of the polyhydrated perchlorates in our study indicating that this vibration does not vary with cation as observed in past transmittance IR studies. However, this band was split into doublets for the anhydrous and tetrahydrated structures. The ν_3 vibrational energies were observed to vary with the polarizing power of the cation such that the vibrational frequency increases with increasing charge/radius (Figure 10). The ν_3 bands in the anhydrous perchlorates and $Ca(ClO_4)_2{\cdot}4H_2O$ spectra were split into doublets, likely due to differences in the ClO_4^- sites in the structures. The ν_3 band in spectra of the anhydrous perchlorates formed a trend of increasing vibrational energy with increasing polarizing power (charge/radius) that was distinct from the trend for the hydrated perchlorates. The Fe^{2+}, Mg, Fe^{3+}, and Al data follow a fairly linear trend, while the Ca data are offset a bit from the others (Figure 10). The ν_3 overtone followed this same

Always consult and cite the final, published document. See http://www.minsocam.org or GeoscienceWorld

trend, but was not observed in the $Ca(ClO_4)_2 \cdot 4H_2O$ spectra. These data confirm the assignment of the band near 2110-2160 cm^{-1} as an overtone of the ν_3 vibration.

In addition to the ClO_4^{2-} vibrations, the hydrated perchlorate spectra (Figure 8) exhibit H_2O bending virbations near 1650 cm^{-1}. This band spans the range of 1635 cm^{-1} for Fe^{3+} perchlorate to 1670 cm^{-1} for Al perchlorate (Table 2) and is dependent on the polarizability of the cation and the degree of hydration of the salt.

The longer wavelength mid-IR perchlorate spectra in our study (Figure 9) exhibited additional features that are not well understood. A doublet feature centered between ~110-215 cm^{-1} (~45-90 μm) is observed for many but not all of the spectra. The position of this doublet does not appear to be correlated with structure or octahedral cation.

Relating Spectral Features to Structure and Composition

Perchlorates exhibit spectral features due to vibrations of the ClO_4^- ion and bound H_2O in the structure. The spectral features observed here are consistent with structural observations from previous studies (e.g. West, 1934; Olmstead et al., 1982; Pascal et al., 1985; Robertson and Bish, 2010). For the hexahydrated perchlorate the structure is based on isolated polyhedra of a metal cation octahedrally coordinated to 6 H_2O molecules and each of these is H-bonded to the ClO_4^- ions. The tetrahydrated perchlorate structure includes isolated clusters of the metal cation octahedrally coordinated to 4 H_2O molecules and 2 ClO_4^- ions. The dihydrate perchlorate structure forms chains of the metal cation bound to 2 H_2O molecules and 4 ClO_4^- ions. The anhydrous perchlorate structure forms an infinite framework of the metal cation coordinated to 6 ClO_4^- ions.

The ClO_4^- bands followed different trends with polarizing power than the H_2O bands. The H_2O stretching bands followed a pattern of decreasing band energy with increasing

Always consult and cite the final, published document. See http://www.minsocam.org or GeoscienceWorld

polarizing power (charge/radius) of the metal cation and the degree of hydration did not appear to greatly influence the vibrational energy of the bands. Thus, the H_2O stretching vibration occurs at different wavelengths for the different perchlorate structures. In contrast, the ClO_4 stretching band energies increased with increasing polarizing power of the metal cation and the degree of hydration influenced these bands as well. Differences in mid-IR band ν_3 stretching vibration energies for anhydrous K and N perchlorates compared with those of hydrated Mg, Fe^{2+}, Fe^{3+} and Al perchlorates are consistent with structural differences. The ν_3 vibrational energy for $Ca(ClO_4)_2{\cdot}4H_2O$ falls in between the other groups indicating this could be intermediate between the other structures.

Spectra of the hydrated Fe^{2+} and Fe^{3+} perchlorates changed significantly upon dehydration through exposure to a low humidity environment or heating to 100 °C. Both samples exhibited color changes as well as changes in the water bands. The Al perchlorate and the $Ca(ClO_4)_2{\cdot}4H_2O$ exhibited some changes due to dehydration, while the anhydrous K and Na samples and hydrated Mg perchlorate did not change under a low humidity environment, but they liquified when heated to 100 °C and exposed to lab air, likely due to water adsorption.

Implications for Mars

The NIR spectral properties of hydrated perchlorates resemble the spectral properties of hydrated sulfates, hydrated phosphates, and zeolites making it difficult to uniquely identify some of these phases. Specifically, the band near 1.9-2.0 μm and the band or drop in reflectance near 2.4 μm found in hydrated perchlorate spectra are both characteristic of the spectra of some sulfates, phosphates and zeolites (e.g., Bishop 2005; Bishop et al. 2012).

Always consult and cite the final, published document. See http://www.minsocam.org or GeoscienceWorld

Features near 1.9-2.0 and 2.4-2.5 μm in CRISM or Observatoire pour la Minéralogie, l'Eau, les Glaces, et l'Activité (OMEGA) spectra of Mars are generally attributed to hydrated sulfates, although some features are more consistent with selected zeolites (Bibring et al. 2005; Murchie et al. 2009). Characterization of the spectral properties of specific perchlorates in this study provides additional data to assist in identifying this mineral group using VNIR remote sensing on Mars. If perchlorates are sufficiently abundant on the surface, then they should be identifiable with CRISM or OMEGA, though they have not yet been identified at the Phoenix landing site (Cull et al. 2010b; Poulet et al. 2010). If perchlorates are present in the soil, near-surface, or inside rocks then these data could enable spectral detection of perchlorates using a VNIR imaging spectrometer on a future landed mission with some digging or scraping ability.

The mid-IR spectral features of perchlorates are related to those of sulfates and phosphates (e.g., Lane and Christensen 1998; Lane 2007). Thus, these data could contribute to detection of salt minerals on Mars using the Thermal Emission Spectrometer (TES) dataset (Christensen et al. 2001).

Analyses of TEGA data from Phoenix and laboratory experiments have shown that thermal decomposition products of perchlorates could react with inorganic carbonates in the soil to release CO_2 in the temperature range 400-680 °C (Cannon et al. 2012). CO_2 release in this temperature range has also been attributed to the possible presence of organic C (Boynton et al. 2009) in soils at the Phoenix landing site. Reaction of perchlorate with organic C has been suggested as one possible explanation for the lack of organic signatures observed by TEGA (Ming et al. 2009).

Always consult and cite the final, published document. See http://www.minsocam.org or GeoscienceWorld

Results from the Sample Analysis at Mars (SAM) instrument on the Mars Science Laboratory (MSL) *Curiosity* rover indicate the presence of Ca perchlorate in the soil at the Rocknest site at Gale Crater, although the hydration level of the perchlorate is not yet known (Archer et al. 2013; Glavin et al. 2013; Leshin et al. 2013). Fe-perchlorates are most consistent with observations at the John Klein and Cumberland sites, although mixtures of Ca- or Mg-perchlorates and Fe oxyhydroxides may also match the data (Ming et al. 2014). Based on laboratory experiments with perchlorate added to Atacama Desert soils, Navarro-Gonzalez et al. (2010) suggested that on Mars, perchlorate could have reacted with putative Martian soil organics to produce some of the results of the Viking gas chromatograph mass spectrometer (Biemann et al. 1977). Other recent experiments have shown that radiation-damaged perchlorate salts can also explain the Viking gas exchange and labeled release experiments (Quinn et al. 2013).

The low thermal decomposition temperatures of Fe^{3+} and Fe^{2+} perchlorate make them unlikely candidates for the type of perchlorate detected by TEGA at the Phoenix site (Hecht et al. 2009) and by SAM at the Rocknest site (Archer et al. 2013; Glavin et al. 2013). Additionally, soil oxidation-reduction potential measurements made using the WCL show that readily soluble iron salt concentrations do not exceed ~ 1 ppm (Quinn et al. 2011) in the soils measured at the Phoenix site. This low solubility of iron perchlorates precludes their presence above trace levels at the Phoenix landing site. However, while *in situ* measurements indicate that Mg and/or Ca perchlorate may be the primary form at the Phoenix (Hecht et al. 2009; Kounaves et al. 2014) and MSL Rocknest sites (Glavin et al. 2013), the presence of other types of perchlorates at other locations on Mars is likely, as

Always consult and cite the final, published document. See http://www.minsocam.org or GeoscienceWorld

indicated by the results of the SAM analyses of sedimentary deposits in Yellowknife Bay (Ming et al. 20134).

The DSC results show that the type of metal cation plays an important role in the patterns of water loss and thermal decomposition. Changes in temperature of the exotherms appear to be related to the perchlorate structure as well as the polarizing power of the cation. Endotherms for water release in the Fe^{2+} and Fe^{3+} perchlorates were both observed at 170 °C. The results of the DSC analyses show that H_2O bond energies in perchlorates depend on the type of cation and hydration state. The highly hygroscopic nature of Ca, Mg, Fe and Al perchlorates observed during our experiments suggest that these salts may be in hydrated forms on the surface or in the near sub-surface of Mars.

The perchlorate abundances observed by Phoenix and MSL are likely too low to be identified from orbit by CRISM, but may be sufficient to be identifiable by a VNIR imager on a future rover. As chloride deposits have been observed from orbit by TES, there may also be regions of elevated perchlorate abundance on the surface that could be detected by TES or CRISM in the future. The data presented here will enable remote sensing searches for perchlorates on the surface of Mars.

Acknowledgements

We are grateful for support from NASA Astrobiology: Exobiology and Evolutionary Biology Program grants NNX09AM93G and NNX13AI67G. We also thank T. Hiroi at Brown University's RELAB for measuring many of the reflectance spectra used in the study and the helpful suggestions from two anonymous reviewers.

Always consult and cite the final, published document. See http://www.minsocam.org or GeoscienceWorld

References

Adams D.M., Blandamer M.J., Symons M.C.R., and Waddington D. (1971) Solvation spectra. Part 39.-Infra-red and Raman studies of aqueous and non-aqueous solutions containing perchlorates. Transactions of the Faraday Society, 67, 611-617.

Archer P.D., Jr., Sutter B., Ming D.W., McKay C.P., Navarro-Gonzalez R., Franz H.B., McAdam A.C., and Mahaffy P.R. (2013) Possible detection of perchlorates by Evolved Gas Analysis of Rocknest Soils: Global implications. Lunar Planet. Sci. Conf. XLIV, The Woodlands, TX, Abstract #2168.

Bao H. and Gu B. (2004) Natural Perchlorate Has a Unique Oxygen Isotope Signature. Environmental science & technology, 38, 5073-5077.

Bibring J.-P., Langevin Y., Gendrin A., Gondet B., Poulet F., Berthé M., Soufflot A., Arvidson R., Mangold N., Mustard J., and Drossart P. (2005) Mars surface diversity as revealed by the OMEGA/Mars Express observations. Science, 307, 1576-1581.

Biemann K. and Bada J.L. (2011) Comment on "Reanalysis of the Viking results suggests perchlorate and organics at midlatitudes on Mars" by Rafael Navarro-González et al. Journal of Geophysical Research: Planets, 116, E12001, doi: 10.1029/2011JE003869.

Biemann K., Oro J., Toulmin III P., Orgel L.E., Nier A.O., Anderson D.M., Simmonds D., Flory P.G., Diaz A.V., Rushneck D.R., Biller J.E., and LaFleur A.L. (1977) The search for organic substances and inorganic volatile compounds in the surface of Mars. Journal of Geophysical Research, 82, 4641-4658.

Bishop J.L. (2005) Hydrated Minerals on Mars. In T. Tokano, Eds., Water on Mars and Life (Advances in Astrobiology and Biogeophysics), p. 65-96. Springer. Berlin.

Bishop J.L. and Murad E. (1996) Schwertmannite on Mars? Spectroscopic analyses of schwertmannite, its relationship to other ferric minerals, and its possible presence in the surface material on Mars. In M. D. Dyar, C. McCammon, and M. W. Schaefer, Eds., Mineral Spectroscopy: A tribute to Roger G. Burns, Special Publication Number 5, p. 337-358. The Geochemical Society. Houston, TX.

Bishop J.L. and Murad E. (2005) The visible and infrared spectral properties of jarosite and alunite. American Mineralogist, 90, 1100-1107.

Always consult and cite the final, published document. See http://www.minsocam.org or GeoscienceWorld

Bishop J.L., Lane M.D., and Dyar M.D. (2012) Reflectance spectra of hydrated sulfates, phosphates and perchlorates. AGU Fall Meet., San Francisco, CA, Abstract P11E-1872.

Bishop J.L., Pieters C.M., Burns R.G., Edwards J.O., Mancinelli R.L., and Froeschl H. (1995) Reflectance spectroscopy of ferric sulfate-bearing montmorillonites as Mars soil analog materials. Icarus, 117, 101-119.

Boynton W.V., Ming D.W., Kounaves S.P., Young S.M.M., Arvidson R.E., Hecht M.H., Hoffmann J., Niles P.B., Hamara D.K., Quinn R.C., Smith P.H., Sutter B., Catling D.C., and Morris R.V. (2009) Evidence for calcium carbonate at the Mars Phoenix Landing Site. Science, 325, 61-64.

Burns R.G. (1993) Mineralogical Applications of Crystal Field Theory. 551. p. Cambridge University Press, Cambridge, UK.

Cannon K.M., Sutter B., Ming D.W., Boynton W.V., and Quinn R. (2012) Perchlorate induced low temperature carbonate decomposition in the Mars Phoenix Thermal and Evolved Gas Analyzer (TEGA). Geophysical Research Letters, 39, L13203, doi: 10.1029/2012gl051952.

Catling D.C., Claire M.W., Zahnle K.J., Quinn R.C., Clark B.C., Hecht M.H., and Kounaves S. (2010) Atmospheric origins of perchlorate on Mars and in the Atacama. Journal of Geophysical Research: Planets, 115, E00E11, doi: 10.1029/2009je003425.

Chen Y., Zhang Y.-H., and Zhao L.-J. (2004) ATR-FTIR spectroscopic studies on aqueous LiClO4, NaClO4, and Mg(ClO4)2 solutions. Physical Chemistry Chemical Physics, 6, 537-542.

Chevrier V.F., Hanley J., and Altheide T.S. (2009) Stability of perchlorate hydrates and their liquid solutions at the Phoenix landing site, Mars. Geophysical Research Letters, 36, L10202, doi: 10.1029/2009gl037497.

Christensen P.R., Bandfield J.L., Hamilton V.E., Ruff S.W., Kieffer H.H., Titus T.N., Malin M.C., Morris R.V., Lane M.D., Clark R.L., Jakosky B.M., Mellon M.T., Pearl J.C., Conrath B.J., Smith M.D., Clancy R.T., Kuzmin R.O., Roush T., Mehall G.L., Gorelick N., Bender K., Murray K., Dason S., Greene E., Silverman S., and Greenfield M. (2001) Mars Global Surveyor Thermal Emission Spectrometer experiment: Investigation description and surface science results. Journal of Geophysical Research, 106, 23,823–23,871.

Always consult and cite the final, published document. See http://www.minsocam.org or GeoscienceWorld

Clark B.C., Baird A.K., Rose Jr. H., Toulmin III P., Christian R.P., Kelliher W.C., Castro A.J., Rowe C.D., Keil K., and Huss G. (1977) The Viking X ray fluorescence experiment: Analytical methods and early results. Journal of Geophysical Research, 82, 4577-4594.

Clark B.C., Morris R.V., McLennan S.M., Gellert R., Jolliff B., Knoll A.H., Squyres S.W., Lowenstein T.K., Ming D.W., Tosca N.J., Yen A., Christensen P.R., Gorevan S., Brückner J., Calvin W., Dreibus G., Farrand W., Klingelhöfer G., Wänke H., Zipfel J., Bell J.F., III, Grotzinger J., McSween H.Y., and Rieder R. (2005) Chemistry and mineralogy of outcrops at Meridiani Planum. Earth and Planetary Sci. Lett., 240, 73-94.

Cull S.C., Arvidson R., Morris R.V., Wolff M., Mellon M.T., and Lemmon M.T. (2010a) Seasonal ice cycle at the Mars Phoenix landing site: 2. Postlanding CRISM and ground observations. Journal of Geophysical Research, 115, E00E19, doi:10.1029/2009JE003410.

Cull S.C., Arvidson R.E., Catalano J.G., Ming D.W., Morris R.V., Mellon M.T., and Lemmon M. (2010b) Concentrated perchlorate at the Mars Phoenix landing site: Evidence for thin film liquid water on Mars. Geophysical Research Letters, 37, 6, doi:201010.1029/2010GL045269.

Davila A.F., Duport L.G., Melchiorri R., Jänchen J., Valea S., de los Rios A., Fairén A.G., Möhlmann D., McKay C.P., Ascaso C., and Wierzchos J. (2010) Hygroscopic salts and the potential for Life on Mars. Astrobiology, 10, 617-628.

Devlin D.J. and Herley P.J. (1987) Thermal decomposition and dehydration of sodium perchlorate monohydrate. Reactivity of Solids, 3, 75-84.

Dyar M.D. and Gunter M.E. (2007) Mineralogy and Optical Mineralogy. 708. p. Mineralogical Society, Chantilly, VA.

Ericksen G.E. (1983) The Chilean nitrate deposits. American Scientist, 71, 366-374.

Gadsden J.A. (1975) Infrared Spectra of Minerals and Related Inorganic Compounds. p. Butterworths

Glavin D.P., Freissinet C., Miller K.E., Eigenbrode J.L., Brunner A.E., Buch A., Sutter B., Archer P.D., Atreya S.K., Brinckerhoff W.B., Cabane M., Coll P., Conrad P.G., Coscia D., Dworkin J.P., Franz H.B., Grotzinger J.P., Leshin L.A., Martin M.G., McKay C., Ming D.W., Navarro-González R., Pavlov A., Steele A., Summons R.E., Szopa C., Teinturier S.,

Always consult and cite the final, published document. See http://www.minsocam.org or GeoscienceWorld

and Mahaffy P.R. (2013) Evidence for perchlorates and the origin of chlorinated hydrocarbons detected by SAM at the Rocknest aeolian deposit in Gale Crater. Journal of Geophysical Research: Planets, 118, 1955-1973.

Glotch T.D., Bandfield J.L., Wolff M.J., and Arnold J.A. (2013) Chloride Salt Deposits on Mars — No Longer "Putative". Lunar Planet. Sci. Conf. XLIV, The Woodlands, TX, Abstract #1549.

Glotch T.D., Bandfield J.L., Tornabene L.L., Jensen H.B., and Seelos F.P. (2010) Distribution and formation of chlorides and phyllosilicates in Terra Sirenum, Mars. Geophysical Research Letters, 37, 1-5.

Gough R.V., Chevrier V.F., Baustian K.J., Wise M.E., and Tolbert M.A. (2011) Laboratory studies of perchlorate phase transitions: Support for metastable aqueous perchlorate solutions on Mars. Earth and Planetary Science Letters, 312, 371-377.

Hanley J., Chevrier V.F., Dalton J.B., and Jamieson C.S. (2011) Reflectance spectra of low-temperature chloride and perchlorate hydrates relevant to planetary remote sensing. 42nd Lunar and Planetary Science Conference, The Woodlands, TX, Abstr. #2327.

Hanley J., Chevrier V., Davis B., Altheide T., and Francis A. (2010) Reflectance spectra of low-temperature chloride and perchlorate hydrates and their relevance to the martian surface. 41st Lunar and Planetary Science Conference, The Woodlands, TX, Abstr. #1953.

Hecht M.H., Kounaves S.P., Quinn R.C., West S.J., Young S.M.M., Ming D.W., Catling D.C., Clark B.C., Boynton W.V., Hoffmann J., DeFlores L.P., Gospodinova K., Kapit J., and Smith P.H. (2009) Detection of perchlorate and the soluble chemistry of Martian soil at the Phoenix Lander site. Science, 325, 64-67.

Horgan B., Kahmann-Robinson J.A., Bishop J.L., and Christensen P.R. (2013) Habitable paleoenvironments preserved in pedogenically altered clay-rich sediments at Mawrth Vallis, Mars. European Planetary Science Congress, London, Abstr. #511.

Huheey J.E., Keiter E.A., and Keiter R.L. (1993) Inorganic Chemistry. Principles of Structure and Reactivity. 964. p. Harper Collins, New York.

Always consult and cite the final, published document. See http://www.minsocam.org or GeoscienceWorld

Jackson W.A., Davila A.F., Estrada N., Berry Lyons W., Coates J.D., and Priscu J.C. (2012) Perchlorate and chlorate biogeochemistry in ice-covered lakes of the McMurdo Dry Valleys, Antarctica. Geochimica et Cosmochimica Acta, 98, 19-30.

Jensen H.B. and Glotch T.D. (2011) Investigation of the near-infrared spectral character of putative Martian chloride deposits. Journal of Geophysical Research: Planets, 116, E00J03, doi: 10.1029/2011je003887.

Kanno H. and Hiraishi J. (1981) Existence of ''nearly free'' hydrogen bonds in glassy aqueous calcium perchlorate solutions. chemical Physical Letters, 83, 452-454.

Kloprogge J.T., Wharton D., Hickey L., and Frost R.L. (2002) Infrared and Raman study of interlayer anions CO32−, NO3−, SO42− and ClO4− in Mg/Al-hydrotalcite. American Mineralogist, 87, 623-629.

Kounaves S.P., Folds K.E., Hansen V.M., Weber A.W., Carrier B.L., and Chaniotakis N.A. (2012) Identity of the perchlorate parent salt(s) at the Phoenix Mars Landing Site based on reanalysis of the calcium sensor response. AGU Fall Meet., San Francisco, CA, Abstract P14B-08.

Kounaves S.P., Chaniotakis N.A., Chevrier V.F., Carrier B.L., Folds K.E., Hansen V.M., McElhoney K.M., O'Neil G.D., and Weber A.W. (2014) Identification of the perchlorate parent salts at the Phoenix Mars landing site and possible implications. Icarus, 232, 226-231.

Kounaves S.P., Stroble S.T., Anderson R.M., Moore Q., Catling D.C., Douglas S., McKay C.P., Ming D.W., Smith P.H., Tamppari L.K., and Zent A.P. (2010a) Discovery of Natural Perchlorate in the Antarctic Dry Valleys and Its Global Implications. Environmental science & technology, 44, 2360-2364.

Kounaves S.P., Hecht M.H., Kapit J., Gospodinova K., DeFlores L., Quinn R.C., Boynton W.V., Clark B.C., Catling D.C., Hredzak P., Ming D.W., Moore Q., Shusterman J., Stroble S., West S.J., and Young S.M.M. (2010b) Wet Chemistry experiments on the 2007 Phoenix Mars Scout Lander mission: Data analysis and results. Journal of Geophysical Research: Planets, 115, E00E10, doi: 10.1029/2009JE003424.

Lane M.D. (2007) Mid-infrared emission spectroscopy of sulfate and sulfate-bearing minerals. American Mineralogist, 92, 1-18.

Always consult and cite the final, published document. See http://www.minsocam.org or GeoscienceWorld

Lane M.D. and Christensen P.R. (1998) Thermal infrared emission spectroscopy of salt minerals predicted for Mars. Icarus, 135, 528-536.

Leshin L.A., Mahaffy P.R., Webster C.R., Cabane M., Coll P., Conrad P.G., Archer P.D., Atreya S.K., Brunner A.E., Buch A., Eigenbrode J.L., Flesch G.J., Franz H.B., Freissinet C., Glavin D.P., McAdam A.C., Miller K.E., Ming D.W., Morris R.V., Navarro-González R., Niles P.B., Owen T., Pepin R.O., Squyres S., Steele A., Stern J.C., Summons R.E., Sumner D.Y., Sutter B., Szopa C., Teinturier S., Trainer M.G., Wray J.J., Grotzinger J.P., and Team M.S. (2013) Volatile, isotope, and organic analysis of Martian fines with the Mars Curiosity rover. Science, 341, doi: 10.1126/science.1238937.

Lewis D.L., Estes E.D., and Hodgson D.J. (1975) The infrared spectra of coordinated perchlorates. Journal of Crystal and Molecular Structure, 5, 67-74.

Marion G.M., Catling D.C., Zahnle K.J., and Claire M.W. (2010) Modeling aqueous perchlorate chemistries with applications to Mars. Icarus, 207, 675-685.

McMillan P.F. and Hofmeister A.M. (1988) Infrared and Raman spectroscopy. In F. C. Hawthorne, Eds., Spectroscopic Methods in Mineralogy and Geology, p. 99-159. Mineralogical Society of America. Washington DC.

Michalski G., Böhlke J.K., and Thiemens M. (2004) Long term atmospheric deposition as the source of nitrate and other salts in the Atacama Desert, Chile: New evidence from mass-independent oxygen isotopic compositions. Geochimica et Cosmochimica Acta, 68, 4023-4038.

Michalski J.R., Cuadros J., Dekov V.M., Bishop J.L., Fiore S., and Dyar M.D. (2013) Constraints on the crystal chemistry of Martian clays from infrared spectroscopy of analogue materials. European Planetary Science Congress, London, Abstr. #1089.

Miller F.A. and Wilkins C.H. (1952) Infrared spectra and characteristic frequencies of inorganic ions. Analytical Chemistry, 24, 1253-1294.

Miller F.A., Carlson G.L., Bentley F.F., and Jones W.H. (1960) Infrared spectra of inorganic ions in the cesium bromide region (700-300 cm-1). Spectrochim. Acta, 16, 135-235.

Ming D.W., Lauer Jr. H.V., Archer Jr. P.D., Sutter B., Golden D.C., Morris R.V., Niles P.B., and Boynton W.V. (2009) Combustion of organic molecules by the thermal decomposition of perchlorate salts: Implications for organics at the Mars Phoenix Scout Landing Site. Lunar Planet Science Conf, LPI-Houston, Abstract #2241.

Always consult and cite the final, published document. See http://www.minsocam.org or GeoscienceWorld

Ming D.W., Archer P.D., Glavin D.P., Eigenbrode J.L., Franz H.B., Sutter B., Brunner A.E., Stern J.C., Freissinet C., McAdam A.C., Mahaffy P.R., Cabane M., Coll P., Campbell J.L., Atreya S.K., Niles P.B., Bell J.F., Bish D.L., Brinckerhoff W.B., Buch A., Conrad P.G., Des Marais D.J., Ehlmann B.L., Fairén A.G., Farley K., Flesch G.J., Francois P., Gellert R., Grant J.A., Grotzinger J.P., Gupta S., Herkenhoff K.E., Hurowitz J.A., Leshin L.A., Lewis K.W., McLennan S.M., Miller K.E., Moersch J., Morris R.V., Navarro-González R., Pavlov A.A., Perrett G.M., Pradler I., Squyres S.W., Summons R.E., Steele A., Stolper E.M., Sumner D.Y., Szopa C., Teinturier S., Trainer M.G., Treiman A.H., Vaniman D.T., Vasavada A.R., Webster C.R., Wray J.J., Yingst R.A., and Team M.S. (2014) Volatile and Organic Compositions of Sedimentary Rocks in Yellowknife Bay, Gale Crater, Mars. Science, 343, doi: 10.1126/science.1245267.

Morris R.V., Golden D.C., Ming D.W., Graff T.G., Arvidson R.E., Wiseman S.M., and Lichtenberg K.A. (2009) Visible and near-IR reflectance spectra for smectite, sulfate and perchlorate under dry conditions for interpretation of martian surface mineralogy. Lunar and Planetary Science Conference, LPI, Houston, abs. #2317.

Murchie S.L., Mustard J.F., Ehlmann B.L., Milliken R.E., Bishop J.L., McKeown N.K., Noe Dobrea E.Z., Seelos F.P., Buczkowski D.L., Wiseman S.M., Arvidson R.E., Wray J.J., Swayze G.A., Clark R.N., Des Marais D.J., McEwen A.S., and Bibring J.P. (2009) A synthesis of Martian aqueous mineralogy after 1 Mars year of observations from the Mars Reconnaissance Orbiter. Journal of Geophysical Research, 114, doi:10.1029/2009JE003342.

Navarro-González R., Vargas E., de la Rosa J., Raga A.C., and McKay C.P. (2010) Reanalysis of the Viking results suggests perchlorate and organics at midlatitudes on Mars. Journal of Geophysical Research: Planets, 115, E12010, doi: 10.1029/2010je003599.

Nebgen J.W., McElroy A.D., and Klodowski H.F. (1966) Raman and Infrared spectra of nitronium perchlorateEds., Studies of Complex Perchlorates, p. 1-13. Callery Chemical Company. Callery, PA.

Nuding D., Gough R.V., Chevrier V.F., and Tolbert M.A. (2013) Deliquescence of calcium perchlorate: An investigation of stable aqueous solutions relevant to Mars. . Lunar Planet Sci. Conf., The Woodlands, TX, abs. #2584.

Always consult and cite the final, published document. See http://www.minsocam.org or GeoscienceWorld

Olmstead M.M., Musker W.K., and Kessler R.M. (1982) Differences in the coordinating ability of water, perchlorate and tetrafluoroborate toward copper(I). The x-ray crystal structures of [Cu(1,4-thioxane)3OClO3], [Cu(1,4-thioxane)3OH2]BF4 and [Cu(1,4-thioxane)4BF4. Transition Metal Chemistry, 7, 140-146.

Osterloo M.M., Anderson F.S., Hamilton V.E., and Hynek B.M. (2010) Geologic context of proposed chloride-bearing materials on Mars. Journal of Geophysical Research, 115, E10012: doi:10.1029/2010JE003613.

Osterloo M.M., Hamilton V.E., Bandfield J.L., Glotch T.D., Baldridge A.M., Christensen P.R., Tornabene L.L., and Anderson F.S. (2008) Chloride-bearing materials in the southern highlands of Mars. Science, 319, 1651-1654.

Parker D.R. (2009) Perchlorate in the environment: the emerging emphasis on natural occurrence. Environmental Chemistry, 6, 10-27.

Parro V., de Diego-Castilla G., Moreno-Paz M., Blanco Y., Cruz-Gil P., Rodríguez-Manfredi J.A., Fernández-Remolar D., Gómez F., Gómez M.J., Rivas L.A., Demergasso C., Echeverría A., Urtuvia V.N., Ruiz-Bermejo M., García-Villadangos M., Postigo M., Sánchez-Román M., Chong-Díaz G., and Gómez-Elvira J. (2011) A Microbial Oasis in the Hypersaline Atacama Subsurface Discovered by a Life Detector Chip: Implications for the Search for Life on Mars Astrobiology, 11, 969-996.

Pestova O.N., Myund L.A., Khripun M.K., and Prigaro A.V. (2005) Polythermal Study of the Systems M(ClO4)2-H2O (M2+ = Mg2+, Ca2+, Sr2+, Ba2+). Russian Journal of Applied Chemistry, 78, 409-413.

Pieters C.M. (1983) Strength of mineral absorption features in the transmitted component of near-infrared reflected light: First results from RELAB. Journal of Geophysical Research, 88, 9534-9544.

Poulet F., Arvidson R.E., Bibring J.P., Gondet B., Jouglet D., Langevin Y., and Morris R.V. (2010) Mineralogy of the Phoenix landing site from OMEGA observations and how that relates to in situ Phoenix measurements. Icarus, 205, 712-715.

Quinn R.C., Chittenden J.D., Kounaves S.P., and Hecht M.H. (2011) The oxidation-reduction potential of aqueous soil solutions at the Mars Phoenix landing site. Geophysical Research Letters, 38, L14202, doi: 10.1029/2011GL047671.

Always consult and cite the final, published document. See http://www.minsocam.org or GeoscienceWorld

Quinn R.C., Martucci H.F.H., Miller S.R., Bryson C.E., Grunthaner F.J., and Grunthaner P.J. (2013) Perchlorate radiolysis on Mars and the origin of Martian soil reactivity. Astrobiology, 13, in press.

Renno N.O., Bos B.J., Catling D., Clark B.C., Drube L., Fisher D., Goetz W., Hviid S.F., Keller H.U., Kok J.F., Kounaves S.P., Leer K., Lemmon M., Madsen M.B., Markiewicz W.J., Marshall J., McKay C., Mehta M., Smith M., Zorzano M.P., Smith P.H., Stoker C., and Young S.M.M. (2009) Possible physical and thermodynamical evidence for liquid water at the Phoenix landing site. Journal of Geophysical Research, 114, 11, doi:10.1029/2009JE003362.

Robertson K. and Bish D. (2010) Determination of the crystal structure of magnesium perchlorate hydrates by X-ray powder diffraction and the charge-flipping method. Acta Crystallographica Section B, 66, 579-584.

Robertson K. and Bish D. (2011) Stability of phases in the Mg(ClO4)2·nH2O system and implications for perchlorate occurrences on Mars. Journal of Geophysical Research: Planets, 116, E07006, doi: 10.1029/2010JE003754.

Ross S.D. (1962) Forbidden transitions in the infra-red spectra of some tetrahedral anions - I. Perchlorates. Spectrochim. Acta, 18, 225-228.

Ross S.D. (1972) Inorganic Infrared and Raman Spectra. p. McGraw-Hill, London.

Schuttlefield J.D., Sambur J.B., Gelwicks M., Eggleston C.M., and Parkinson B.A. (2011) Photooxidation of chloride by oxide minerals: Implications for perchlorate on Mars. Journal of the American Chemical Society, 133, 17521-17523.

Skogareva L.S., Shilov G.V., and Karelin A.I. (2012) Crystal structure and Raman spectra of [Fe(H2O)6]3+(ClO 4 −)3·3H2O. Journal of Structural Chemistry, 53, 907-914.

Solovyov L.A. (2012) Revision of the Mg(ClO4)2.4H2O crystal structure. Acta Crystallographica Section B, 68, 89-90.

Sowe M., Bishop J.L., Gross C., and Walter S. (2013) Deposits of the Peruvian Pisco Formation compared to layered deposits on Mars. European Planetary Science Congress, London, Abstr. #990.

Telser J., van Slageren J., Vongtragool S., Dressel M., Reiff W.M., Zvyagin S.A., Ozarowski A., and Krzystek J. (2005) High-frequency/high-field EPR spectroscopy of the high-spin

Always consult and cite the final, published document. See http://www.minsocam.org or GeoscienceWorld

ferrous ion in hexaaqua complexes. Magnetic Resonance in Chemistry, 43, S130-S139.

Weitz C.M., Bishop J.L., and Grant J.A. (2013) Gypsum, opal, and fluvial channels within a trough of Noctis Labyrinthus, Mars: Implications for aqueous activity during the Late Hesperian to Early Amazonian. Planet. Space Sci, 87, 130-145.

West C.D. (1935) Crystal structures of hydrated compounds, II. Structure type Mg(ClO4)2•6H2O. Z. Kristallogr., 91, 480-493.

White M.A. and Falk M. (1986) Phase transitions in M(ClO4)2 . 6H2O (M=Mg, Zn). Investigations by adiabatic calorimetry and infrared spectroscopy. The Journal of Chemical Physics, 84, 3484-3490.

Wray J.J., Murchie S.L., Squyres S.W., Seelos F.P., and Tornabene L.L. (2009) Diverse aqueous environments on ancient Mars revealed in the southern highlands. Geology, 39, 1043-1046.

Always consult and cite the final, published document. See http://www.minsocam.org or GeoscienceWorld

Table 1 Summary of mid-IR absorptions in transmittance spectra of perchlorates (ClO_4) and chlorates (ClO_3) from the literature

Vibrational bands in cm^{-1}		$KClO_4$	$NaClO_4 \cdot H_2O$	$NaClO_4 \cdot 2H_2O$	$Ca(ClO_4)_2 \cdot 4H_2O$	Mg $(ClO_4)_2$*	$Mg(ClO_4)_2 \cdot 6H_2O$	$Fe^{2+}(ClO_4)_2 \cdot 6H_2O$	$KClO_3$	$NaClO_3$
asymmetric stretch	ν_3	1075-1093		1081	1087	1060	sh 1087			990
		1111	1100	1111	1111	1130	1111	1111	962	965
		1140-1143		1124	1139		wsh 1143			
symmetric stretch	ν_1	940-941		939	939	945	940	943	938	935
						962				
asymmetric bend	ν_4	625-627	624	625	627	622	627	628	623	627
symmetric bend	ν_2		480			495			490	484
						460				

Band assignments from Miller and Wilkins, 1952; Miller et al., 1960; Ross, 1962. *H_2O molecules were not indicated to be present in this sample, but a H_2O bending vibration is observed as in the spectra of the Na $ClO_4 \bullet H_2O$ sample. Sh indicates shoulder and wsh indicates weak shoulder.

Table 2 Summary of Spectral Features for Perchlorates from reflectance spectra in this study

	Anhydrous $KClO_4$	Anhydrous $NaClO_4$	$Ca(ClO_4)_2 \cdot 4H_2O$	$Mg(ClO_4)_2 \cdot nH_2O$	$Fe^{2+}(ClO_4)_2 \cdot nH_2O$	$Fe^{3+}(ClO_4)_3 \cdot nH_2O$	$Al(ClO_4)_3 \cdot 9H_2O$
Electronic excitations in µm (and cm^{-1})							
					~0.95-1.1 (~9000-10,500)	0.767 (~13,000)	
NIR bands in µm (and cm^{-1})							
			1.423 (7030)	1.435 (6970)	1.439 (6950)	1.472 (6790)	1.476 (6775)
			1.750 (5715)				
			1.803 (5550)				
			1.93 (5180)	1.93 (5180)	1.94 (5155)	1.99 (5025)	1.98 (5050)
			2.15 (4650)	2.16 (4630)	2.16 (4630)	2.18 (4585)	
			~2.4 (~4170)	2.41 (4150)	2.4 (~4170)	2.45 (4080)	2.39 (4185)
H_2O stretch			2.74, 2.79 (3655,3585)	2.77 (3610)	2.77 (3615)	2.83 (3530)	2.84 (3540)
3X ν_3	3.22 (3105)	3.17 (3150)					
3X ν_3	3.90 (2950)	3.34 (2995)					
2X $\nu_3 + \nu_4$	3.79 (2640)	3.75 (2670)	3.64 (2750)	3.66 (2730)			
2X $\nu_3 + \nu_4$	4.00 (2500)	3.98 (2515)	3.87 (2585)	3.88 (2575)			
2X ν_3	4.57, 4.95 (2190, 2020) (2135, split)	4.47, 4.87 (2235, 2055) (2160, split)		4.52, 4.96 (2210, 2015) (2115, split)	4.52, 4.93 (2210, 2030) (2115, split)	4.33, 4.93 (2310, 2030) (2130, split)	4.15, 4.90 (2410, 2040) (2140, split)
mid-IR peaks in cm^{-1} (and µm)							
	1870 (split) (5.35)	1900 (5.26)					
$\nu_3 + \nu_4$	1750 (split) (5.71)	1760 (split) (5.68)					

Always consult and cite the final, published document. See http://www.minsocam.org or GeoscienceWorld

H_2O bend			1655 (6.04)	1650 (6.06)	1645 (6.07)	1635 (6.12)	1670 (5.99)
$\nu_3 + \nu_4$	1565 (split) (6.39)	1570 (split) (6.37)					
ν_3	1185, 1125 (8.44, 8.89)	1140 (split) (8.77)	1160, 1095 (8.62, 9.13) (1120 split)	1115 (8.97)	1105 (9.05)	1120 (8.93)	1130 (8.85)
ν_1	940[d] (10.6) 885, 825 (11.3, 12.1)	825 (12.1)	980 (10.2)	950[d] (10.5)			
ν_4	630 (15.8) 465 (21.5) (split)	644 (15.5) (split) 485 (20.6) (split) ~115 (87) (split)	630 (15.8) (split) ~215 (46) (split)	630 (15.8) ~210 (48) (split)	630 (15.8) 350 ~125 (80) (split)	630 (15.8) 500	630 (15.8) 460 ~110 (90) (split)
Radius (Å)*	1.52	1.16	1.14	0.860	0.920	0.785	0.675
Charge/radius*	0.66	0.86	1.75	2.33	2.17	3.82	4.44

Split indicates that the spectral feature is plit into two or more bands; d indicates downward band instead of upward peak at longer wavelegnths; *effective ionic radii from Huheey et al. (1993) assuming octahedral coordination of the cation and high spin state for Fe^{2+} and Fe^{3+} (Telser et al. 2005; Sowe et al. 2013).

Always consult and cite the final, published document. See http://www.minsocam.org or GeoscienceWorld

Figure Captions

Figure 1. Close-up of the Mg coordination polyhedra in $Mg(ClO_4)_2{\cdot}2H_2O$ and $Mg(ClO_4)_2{\cdot}4H_2O$ described by Robertson and Bish (2010) using a combination of an *ab initio* charge-flipping model (e.g, as used in Dyar and Gunter (2007)) based on x-ray powder diffraction data and subsequent fundamental-parameters Rietveld refinement. Oxygen anions are red, Mg^{2+} is yellow, and H^+ is red. The O^{2-} anions that are not part of water molecules are corners of perchlorate anions (see Figure 2).

Figure 2. Changes in the structure of $Mg(ClO_4)_2{\cdot}nH_2O$ perchlorate as thermal decomposition occurs from n = 4 to n = 2, demonstrating the fundamental structural rearrangements that occur. $Mg(ClO_4)_2{\cdot}4H_2O$ contains Mg octahedra, each with two perchlorate anions in the *trans* position. Structural rearrangement occurs in $Mg(ClO_4)_2{\cdot}2H_2O$, which is composed of chains of Mg octahedra linked by perchlorate anions that share two of their four corners.

Figure 3. VNIR reflectance spectra from 0.3 to 5 μm of several perchlorate salts, offset for clarity.

Figure 4. NIR reflectance spectra from 1.2-2.7 μm illustrating variations in the perchlorate spectral features due to changes in the cation. The Mg perchlorate spectrum has a much brighter reflectance in this region and is divided by 2 for this plot.

Always consult and cite the final, published document. See http://www.minsocam.org or GeoscienceWorld

Figure 5. Comparison of vibrational energies (in cm^{-1}) of the H_2O bands with polarizing power of octahedral cations showing that the frequency of these vibrations decreases with increase charge/radius. a) H_2O stretching vibration and its overtone, and b) H_2O stretching vibration and H_2O combination (stretching plus bending) band.

Figure 6. VNIR reflectance spectra measured of perchlorates under variable hydration conditions (ambient, dehydrated and heated): a) Fe^{3+} perchlorate, b) Fe^{2+} perchlorate, and c) Al perchlorate. Note that the heated samples reacted during heating but spectra were measured under ambient conditions after cooling and in many cases they rehydrated.

Figure 7. DSC scans of sodium (Na) and potassium (K) perchlorates (7a), magnesium (Mg) and calcium (Ca) perchlorates (7b), and ferrous (Fe II) and ferric (FeIII) perchlorates (7c). Major transitions are indicated by: P = phase transformation; W = water loss; F= fusion (melting); D = decomposition.

Figure 8. Mid-IR reflectance spectra from 200-2000 cm^{-1} illustrating the dominant vibrational modes near 630 and 1130 cm^{-1}, as well as additional modes for some samples. The hydrated perchlorates with Mg, Fe^{2+}, Fe^{3+} and Al have similar ClO_4^- features due to their related symmetries and an H_2O bending vibration near 1635-1670 cm^{-1}. The anhydrous Na and K perchlorates have multiple strong ClO_4^- bands, some of which are split. The mid-IR spectral features for Ca perchlorate exhibit some similarities with each group suggesting that this Ca perchlorate structure falls in between the structures of the other groups.

Always consult and cite the final, published document. See http://www.minsocam.org or GeoscienceWorld

Figure 9. Mid-IR reflectance spectra from 100-1300 cm^{-1} illustrating variations in the longer wavelength features with type of cation.

Figure 10. Comparison of ClO_4^- ν_3 and ν_3 overtone (OT) band positions (in cm^{-1}) with polarizing power of octahedral cations showing that the frequency of these vibrations increases with increasing charge/radius.

Always consult and cite the final, published document. See http://www.minsocam.org or GeoscienceWorld

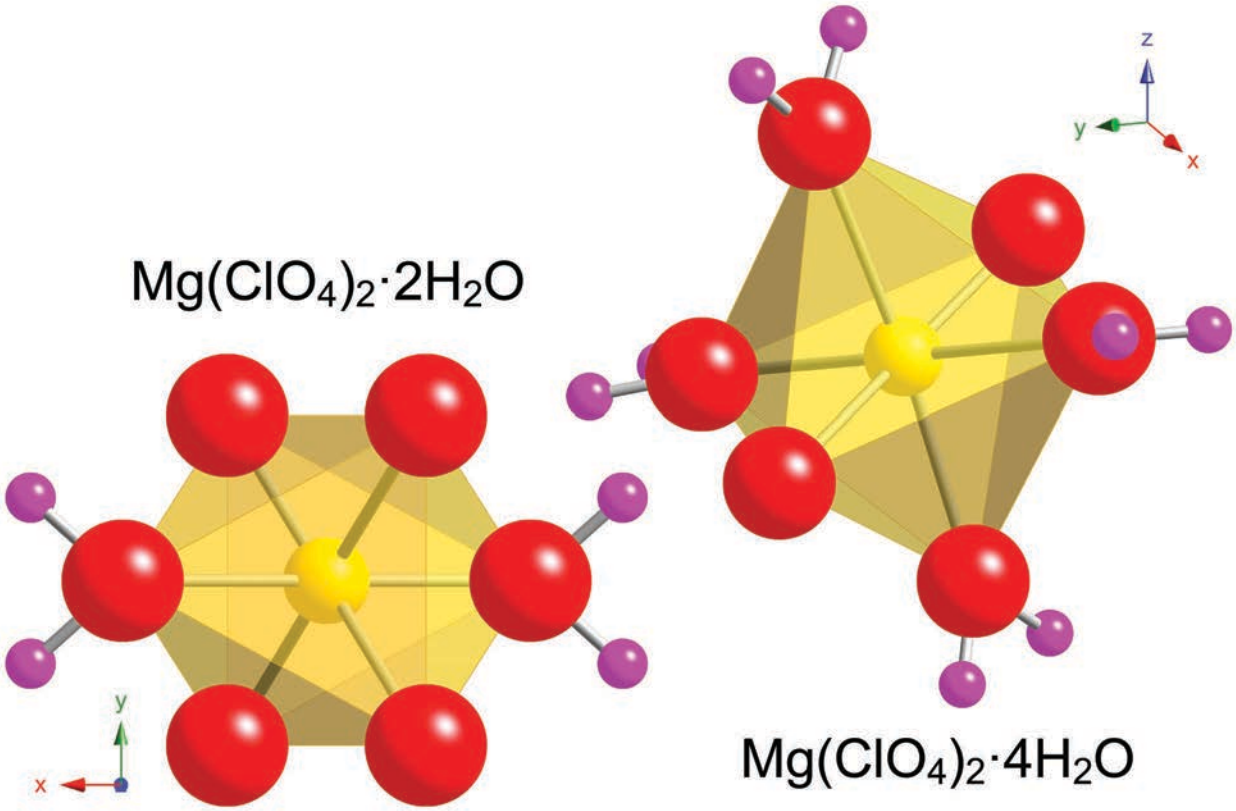

Figure 1. Close-up of the Mg coordination polyhedra in $Mg(ClO_4)_2{\cdot}2H_2O$ and $Mg(ClO_4)_2{\cdot}4H_2O$ described by Robertson and Bish (2010) using a combination of an *ab initio* charge-flipping model (e.g, as used in Dyar and Gunter (2007)) based on x-ray powder diffraction data and subsequent fundamental-parameters Rietveld refinement. Oxygen anions are red, Mg^{2+} is yellow, and H^{+} is red. The O^{2-} anions that are not part of the water molecules are corners of perchlorate anions (see Figure 2).

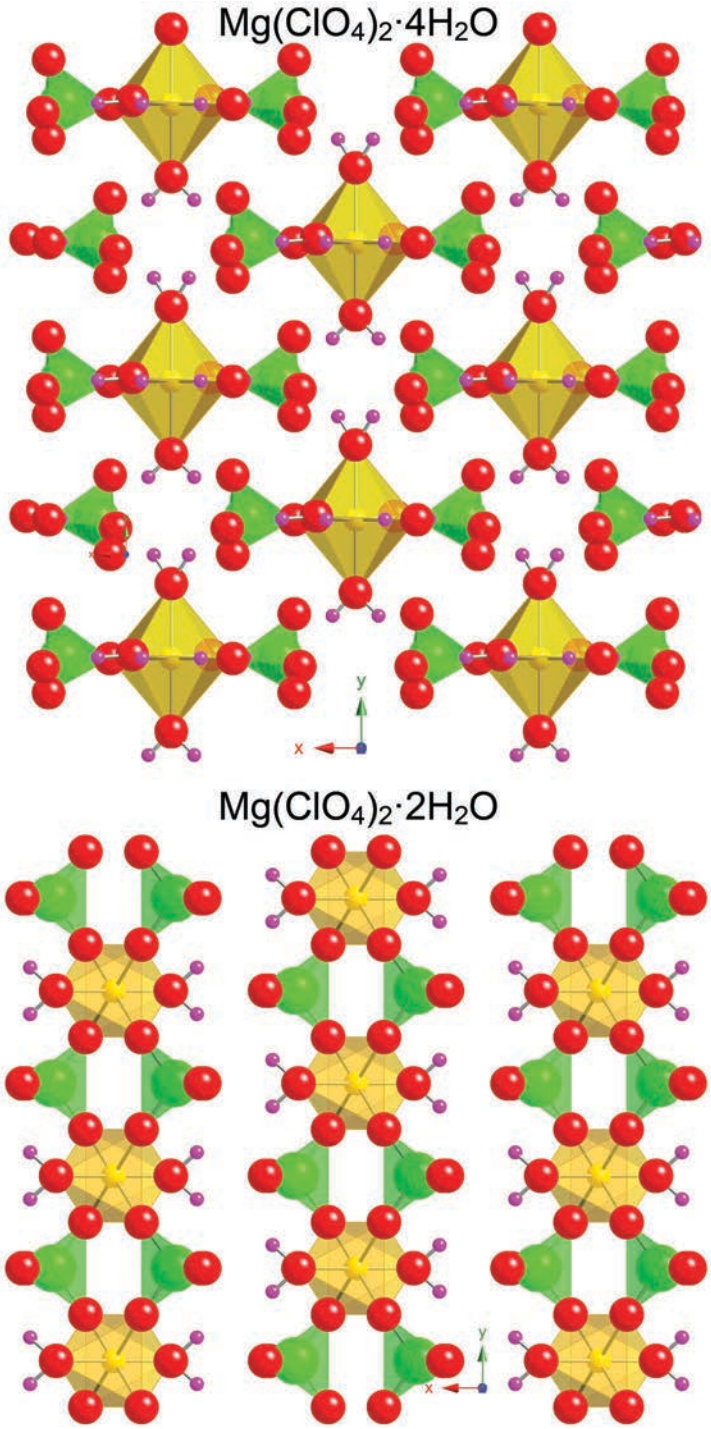

Figure 2. Changes in the structure of $Mg(ClO_4)_2 \cdot nH_2O$ perchlorate as thermal decomposition occurs from $n = 4$ to $n = 2$, demonstrating the fundamental structural rearrangements that occur. $Mg(ClO_4)_2 \cdot 4H_2O$ contains Mg octahedra, each with two perchlorate anions in the *trans* position. Structural rearrangement occurs in $Mg(ClO_4)_2 \cdot 2H_2O$, which is composed of chains of Mg octahedra linked by perchlorate anions that share two of their four corners.

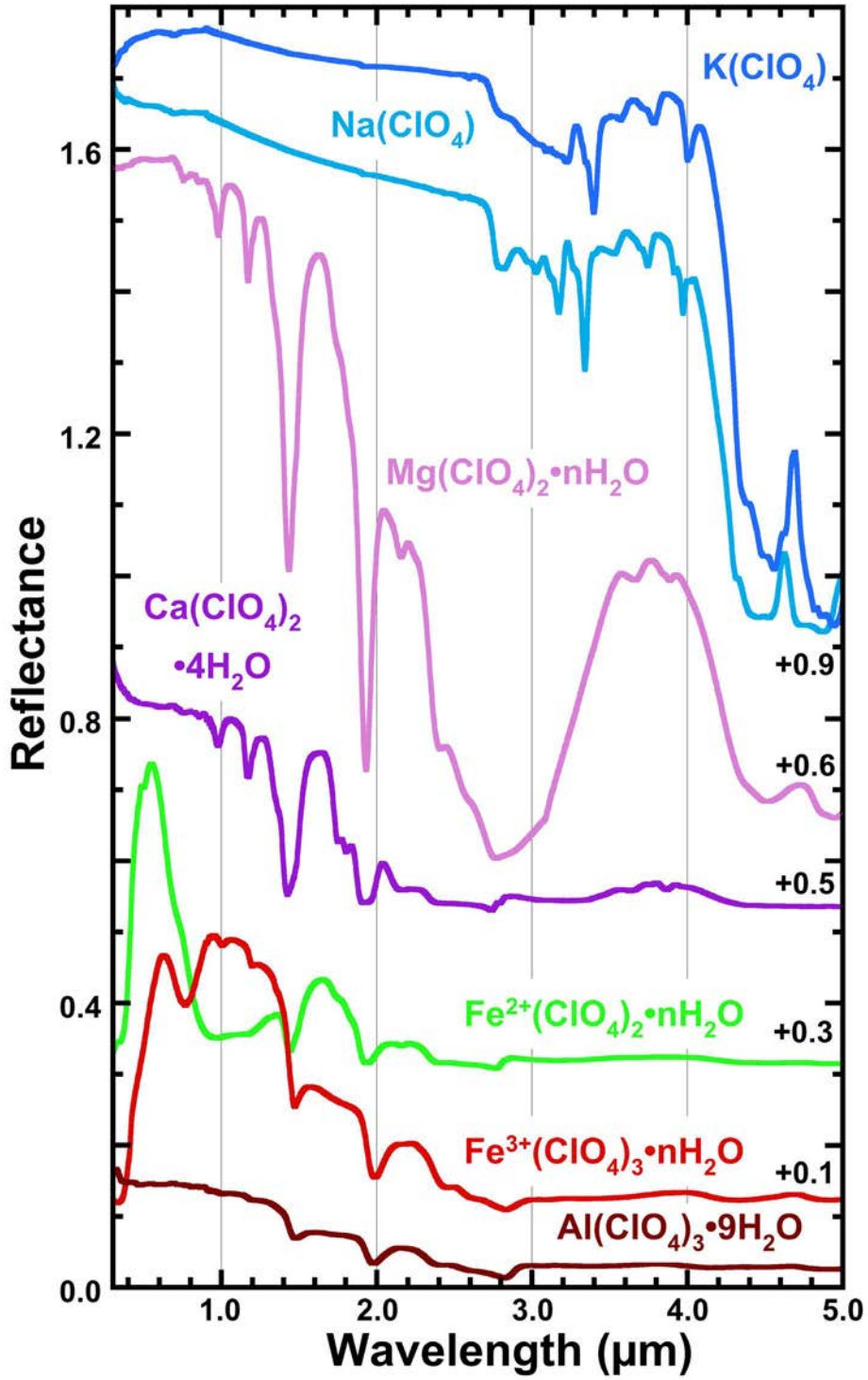

Figure 3. VNIR reflectance spectra from 0.3 to 5 µm of several perchlorate salts, offset for clarity.

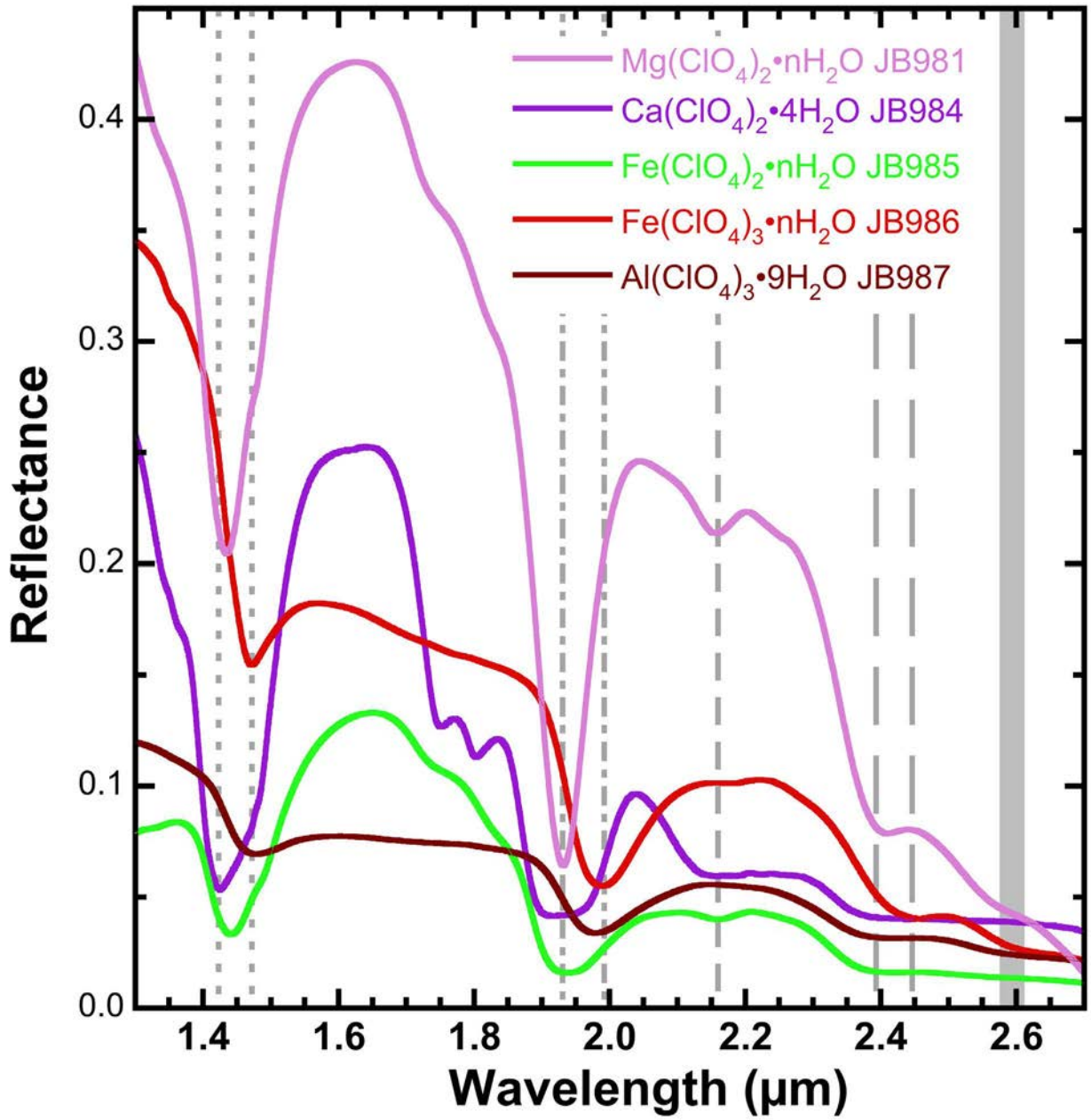

Figure 4. NIR reflectance spectra from 1.2-2.7 μm illustrating variations in the perchlorate spectral features due to changes in the cation. The Mg perchlorate spectrum has a much brighter reflectance in this region and is divided by 2 for this plot.

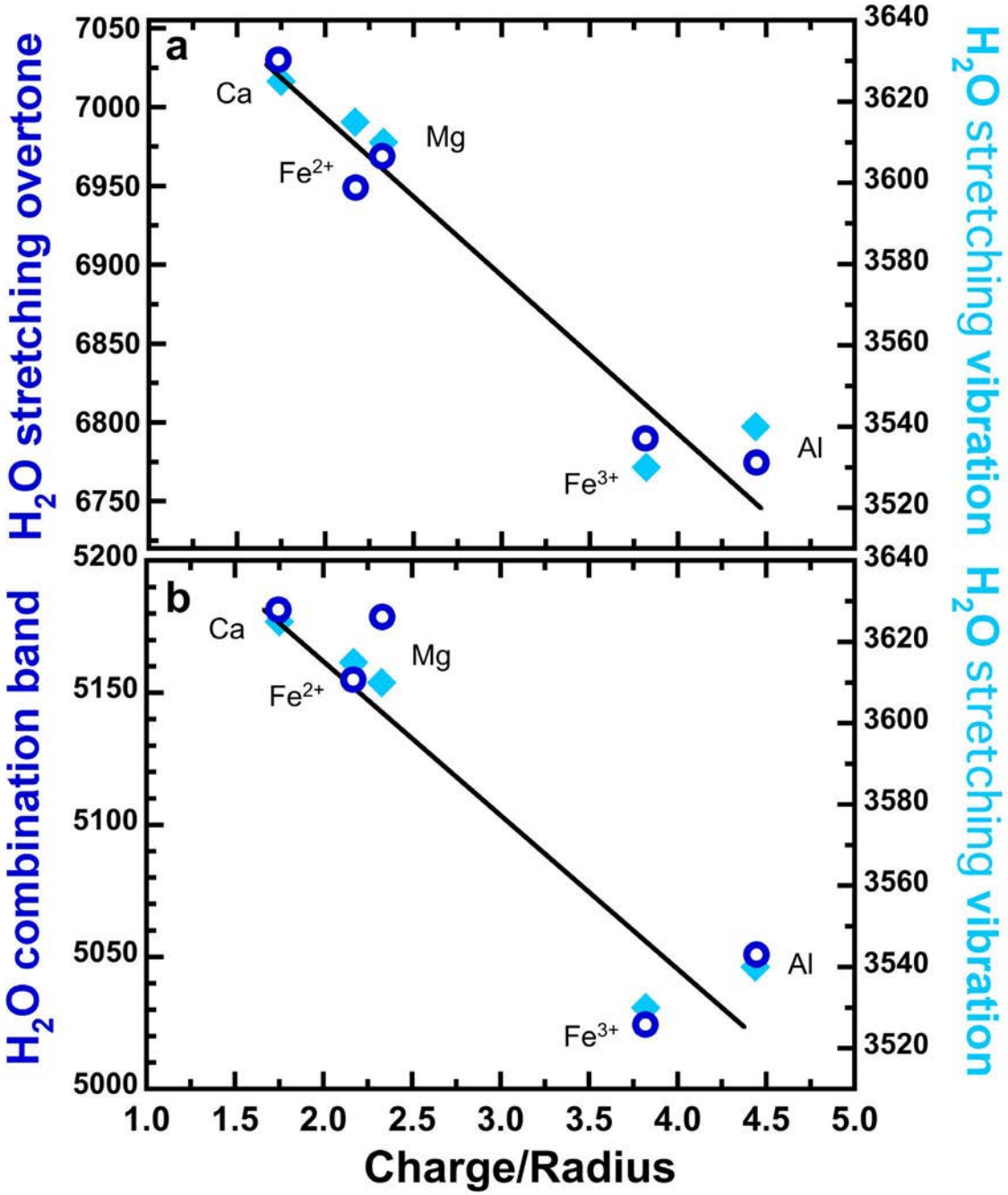

Figure 5. Comparison of vibrational energies (in cm^{-1}) of the H_2O bands with polarizing power of octahedral cations showing that the frequency of these vibrations decreases with increase charge/radius. a) H_2O stretching vibration and its overtone, and b) H_2O stretching vibration and H_2O combination (stretching plus bending) band.

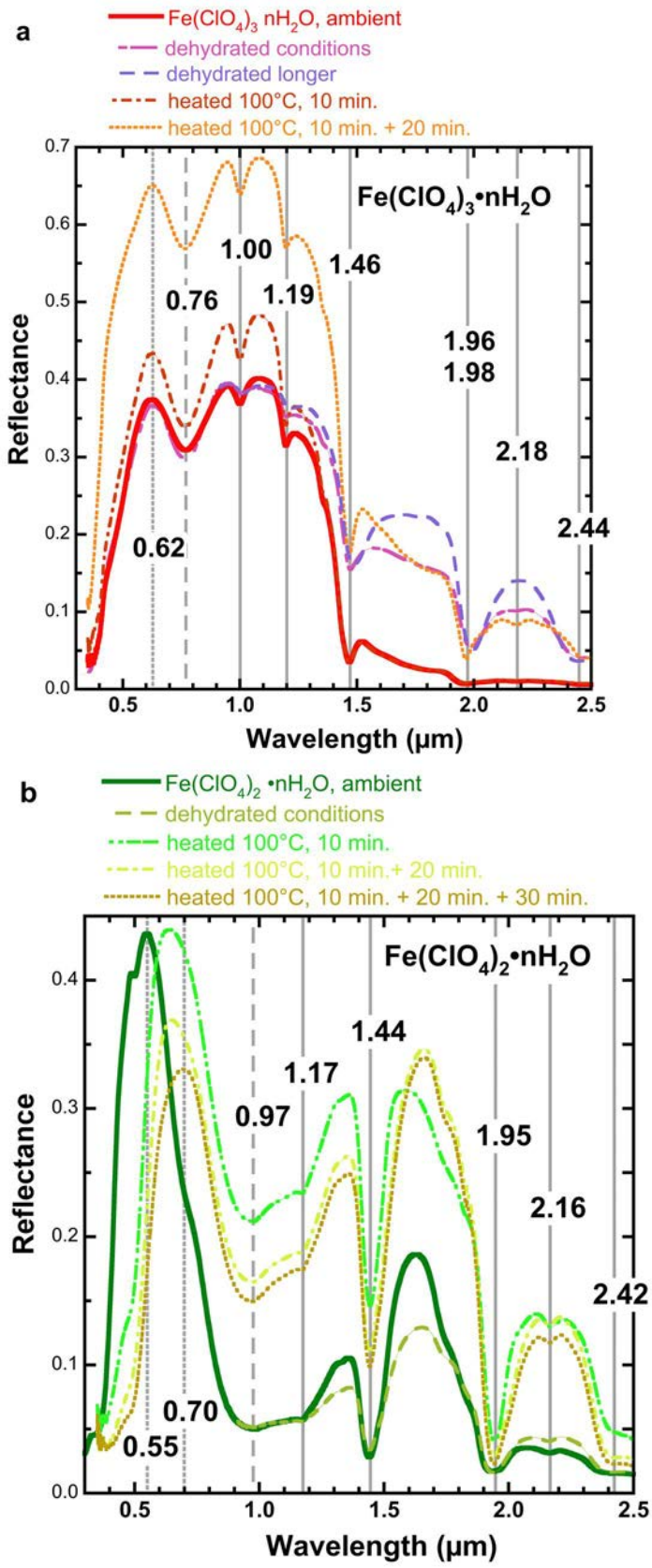
a
Fe(ClO4)3 nH2O, ambient
dehydrated conditions
dehydrated longer
heated 100°C, 10 min.
heated 100°C, 10 min. + 20 min.
Fe(ClO4)3•nH2O
1.00
1.46
0.76
1.19
1.96
1.98
2.18
2.44
0.62
Reflectance
Wavelength (μm)
b
Fe(ClO4)2 •nH2O, ambient
dehydrated conditions
heated 100°C, 10 min.
heated 100°C, 10 min.+ 20 min.
heated 100°C, 10 min. + 20 min. + 30 min.
Fe(ClO4)2•nH2O
1.44
1.17
0.97
1.95
2.16
2.42
0.70
0.55
Reflectance
Wavelength (μm)

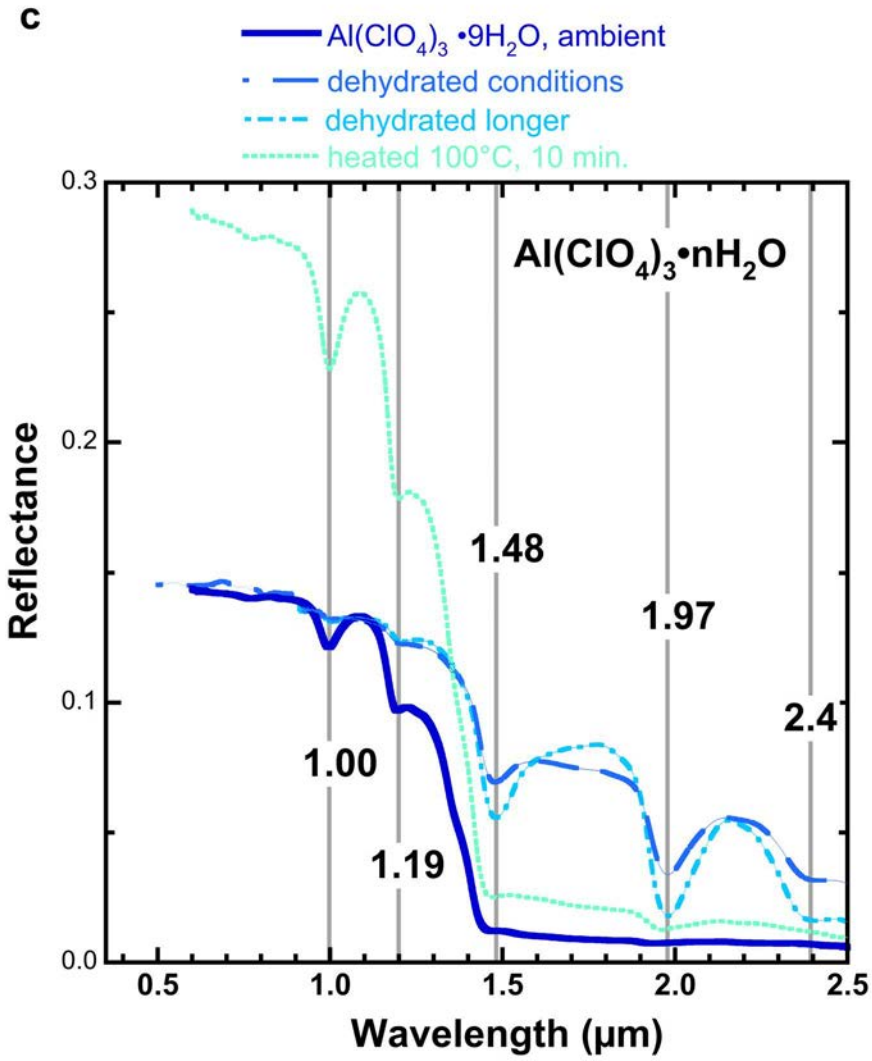

Figure 6. VNIR reflectance spectra measured of perchlorates under variable hydration conditions (ambient, dehydrated and heated): a) Fe^{3+} perchlorate, b) Fe^{2+} perchlorate, and c) Al perchlorate. Note that the heated samples reacted during heating but spectra were measured under ambient conditions after cooling and in many cases they rehydrated.

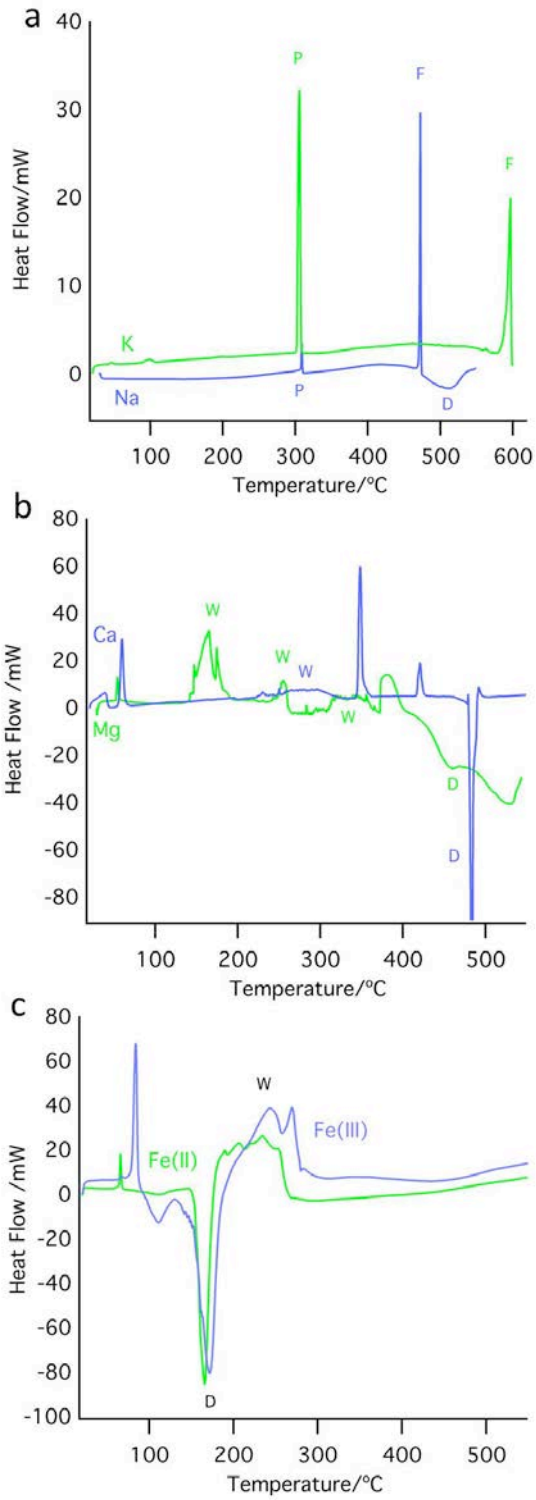

Figure 7. DSC scans of sodium (Na) and potassium (K) perchlorates (7a), magnesium (Mg) and calcium (Ca) perchlorates (7b), and ferrous (Fe II) and ferric (FeIII) perchlorates (7c). Major transitions are indicated by: P = phase transformation; W = water loss; F= fusion (melting); D = decomposition.

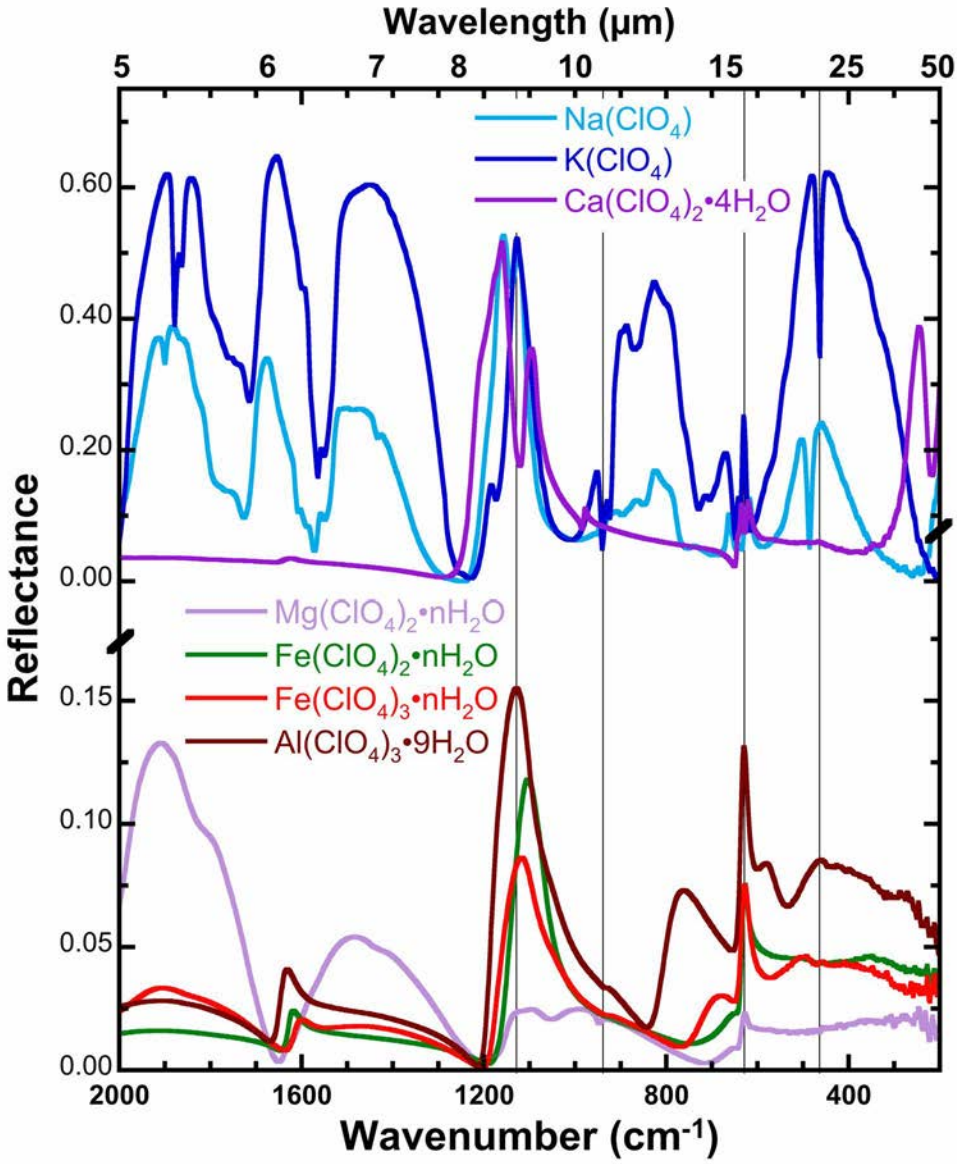

Figure 8. Mid-IR reflectance spectra from 200-2000 cm^{-1} illustrating the dominant vibrational modes near 630 and 1130 cm^{-1}, as well as additional modes for some samples. The hydrated perchlorates with Mg, Fe^{2+}, Fe^{3+} and Al have similar ClO_4^- features due to their related symmetries and an H_2O bending vibration near 1635-1670 cm^{-1}. The anhydrous Na and K perchlorates have multiple strong ClO_4^- bands, some of which are split. The mid-IR spectral features for Ca perchlorate exhibit some similarities with each group suggesting that this Ca perchlorate structure falls in between the structures of the other groups.

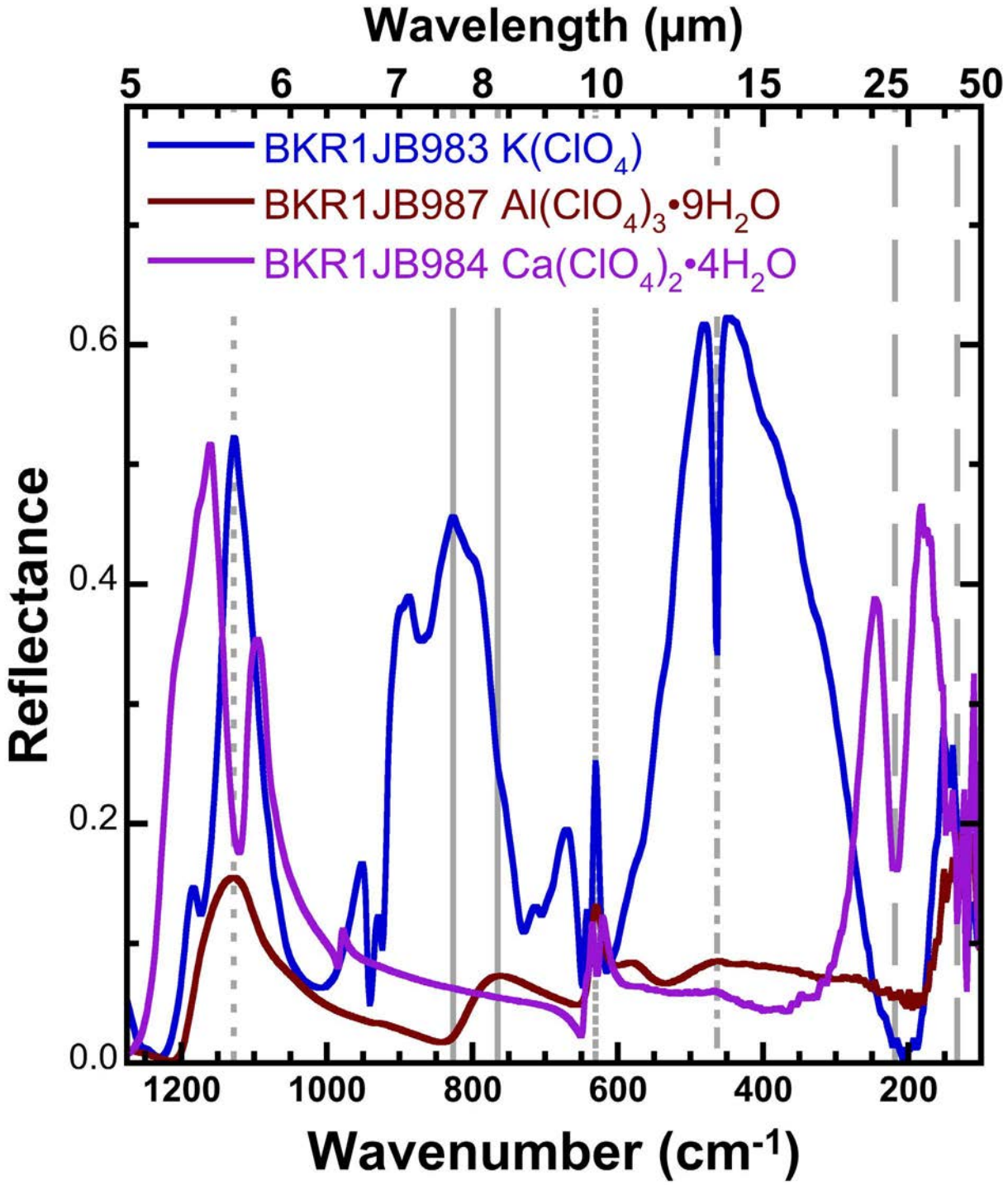

Figure 9. Mid-IR reflectance spectra from 100-1300 cm^{-1} illustrating variations in the longer wavelength features with type of cation.

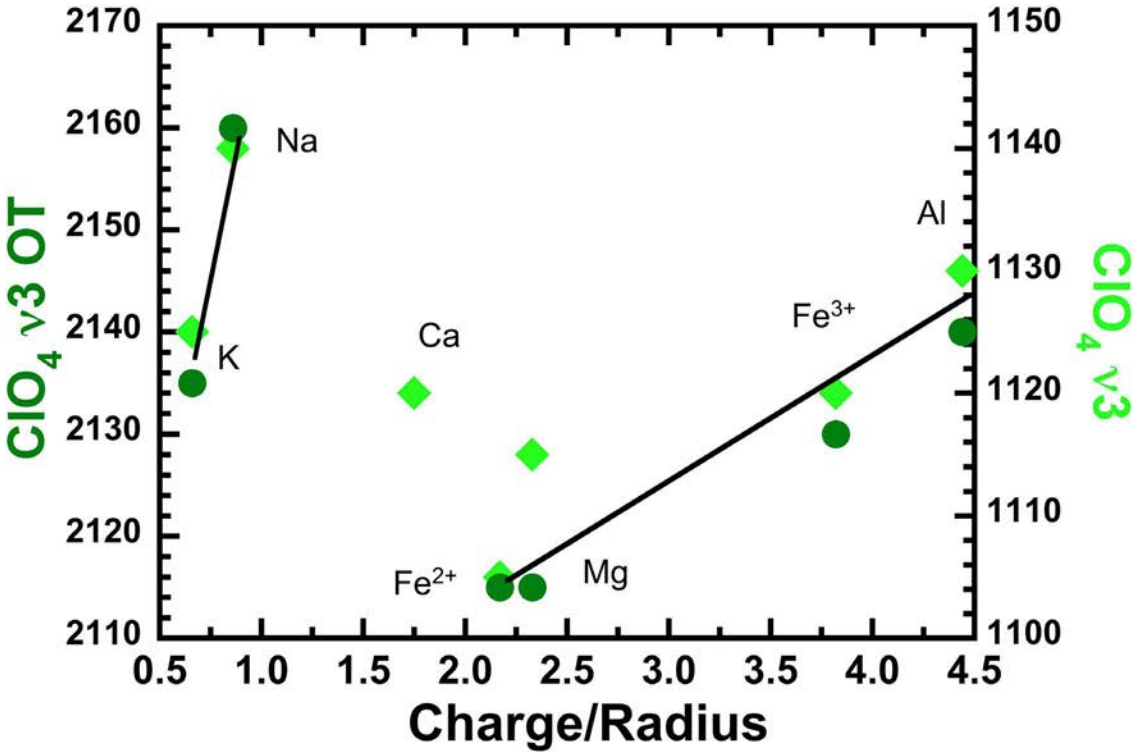

Figure 10. Comparison of ClO_4^- ν_3 and ν_3 overtone (OT) band positions (in cm^{-1}) with polarizing power of octahedral cations showing that the frequency of these vibrations increases with increasing charge/radius.